Describing Function Analysis of Control Systems Containing Multiple Nonlinearities

by

R. E. Lueg

and

V. S. Sohoni

University, Alabama

1967

Acknowledgements

The authors wish to express their gratitude to the National Aeronautics and Space Administration (under NSG-381) and the U.S. Army Missile Command (under contract research) for the financial support which made this study possible.

CONTENTS

	Page
ACKNOWLEDGEMENTS	ii
CONTENTS	iii
LIST OF TABLES	v
LIST OF ILLUSTRATIONS	vi
ABSTRACT	viii
CHAPTER	
I. INTRODUCTION	1
II. DESCRIBING FUNCTION METHODS	3
2.1 Definition	3
2.2 Stability Analysis	5
III. THE DERIVATION OF DESCRIBING FUNCTION FOR TWO MULTIPLE NONLINEARITIES	8
3.1 First Multiple Nonlinearity	8
3.2 Second Multiple Nonlinearity	12
IV. SAMPLE PROBLEMS INDICATING USE OF THE DERIVED DESCRIBING FUNCTION	14
4.1 A Sample Problem Containing First Multiple Nonlinearity	14
4.2 A Sample Problem Containing Second Multiple Nonlinearity	16
V. ACCURACY CONSIDERATIONS AND COMPARISON WITH ANALOG COMPUTER RESULTS	21
VI. TRANSIENT RESPONSE AND CLOSED LOOP FREQUENCY RESPONSE FROM DESCRIBED FUNCTION DATA	23
6.1 Transient Response	23
Finnigan Approach	
Kochenburger Approach	
6.2 Closed Loop Frequency Response	26

CONTENTS (continued)

Page

Gibson's Method

Thaler's Method

DIDF (Input Sinewaves Harmonically Related)

Approximate DIDF, Boyer's Method

VII. CONCLUSIONS 38

APPENDIX

I. COMPUTATION OF y(t), FIRST MULTIPLE NONLINEARITY . . 69

II. COMPUTATION OF z(t), FIRST MULTIPLE NONLINEARITY . . 71

III. DESCRIBING FUNCTION OF THE COMBINED NONLINEARITY OF DEADZONE AND BACKLASH 72

IV. COMPUTATION OF y(t), SECOND MULTIPLE NONLINEARITY . . 75

V. COMPUTATION OF z(t), SECOND MULTIPLE NONLINEARITY . . 78

VI. DESCRIBING FUNCTION OF THE COMBINED NONLINEARITY OF RELAY AND BACKLASH 79

VII. ANALOG COMPUTER SIMULATION I 80

VIII. ANALOG COMPUTER SIMULATION II 82

REFERENCES 84

LIST OF TABLES

Tables		Page
I	$\lvert G_D \rvert$ and ϕ_D for the First Multiple Nonlinearity for $\frac{\delta K}{W} = 1$	40
II	$\lvert G_D \rvert$ and ϕ_D for the First Multiple Nonlinearity for $\frac{\delta K}{W} = 2$	41
III	$\lvert G_D \rvert$ and ϕ_D for the First Multiple Nonlinearity for $\frac{\delta K}{W} = 3$	42
IV	$\lvert G_D \rvert$ and ϕ_D for the First Multiple Nonlinearity for $\frac{\delta K}{W} = 4$	43
V	$\lvert G_D \rvert$ and ϕ_D for the First Multiple Nonlinearity for $\frac{\delta K}{W} = \frac{1}{2}$	44
VI	$\lvert G_D \rvert$ and ϕ_D for the First Multiple Nonlinearity for $\frac{\delta K}{W} = \frac{1}{3}$	45
VII	$\lvert G_D \rvert$ and ϕ_D for the First Multiple Nonlinearity for $\frac{\delta K}{W} = \frac{1}{4}$	46
VIII	$\lvert G_D \rvert$ and ϕ_D for the Second Multiple Nonlinearity for $\frac{K}{W} = 1$	47
IX	$\lvert G_D \rvert$ and ϕ_D for the Second Multiple Nonlinearity for $\frac{K}{W} = 3$	48
X	$\lvert G_D \rvert$ and ϕ_D for the Second Multiple Nonlinearity for $\frac{K}{W} = 5$	49
XI	$\lvert G_D \rvert$ and ϕ_D for the Second Multiple Nonlinearity for $\frac{K}{W} = 7$	50
XII	$\lvert G_D \rvert$ and ϕ_D for the Second Multiple Nonlinearity for $\frac{K}{W} = 9$	51
XIII	$\lvert G_D \rvert$ and ϕ_D for the Second Multiple Nonlinearity for $\frac{K}{W} = 11$	52
XIV	The Analog Results Versus Analytical Results, First Multiple Nonlinearity	80
XV	The Analog Results Versus Analytical Results, Second Multiple Nonlinearity	82

LIST OF ILLUSTRATIONS

FIGURE		Page
1.	A Control System	3
2.	First Multiple Nonlinearity	9
3.	Nonlinearity Equivalent to First Multiple Nonlinearity. .	9
4.	Output of the Deadzone Element.	9
5.	Nichols Plot of First Multiple Nonlinearity, $\delta K/W=1$ . . .	53
6.	Nichols Plot of First Multiple Nonlinearity, $\delta K/W=2$ . . .	54
7.	Nichols Plot of First Multiple Nonlinearity, $\delta K/W=3$ . . .	55
8.	Nichols Plot of First Multiple Nonlinearity, $\delta K/W=4$ . . .	56
9.	Nichols Plot of First Multiple Nonlinearity, $\delta K/W=1/2$ . .	57
10.	Nichols Plot of First Multiple Nonlinearity, $\delta K/W=1/3$ . .	58
11.	Nichols Plot of First Multiple Nonlinearity, $\delta K/W=1/4$ . .	59
12.	Second Multiple Nonlinearity	12
13.	Nonlinearity Equivalent to Second Multiple Nonlinearity .	12
14.	Output of the Relay With Hysteresis	12
15.	Nichols Plot of Second Multiple Nonlinearity, $K/W=1$ . . .	60
16.	Nichols Plot of Second Multiple Nonlinearity, $K/W=3$ . . .	61
17.	Nichols Plot of Second Multiple Nonlinearity, $K/W=5$ . . .	62
18.	Nichols Plot of Second Multiple Nonlinearity, $K/W=7$ . . .	63
19.	Nichols Plot of Second Multiple Nonlinearity, $K/W=9$ . . .	64
20.	Nichols Plot of Second Multiple Nonlinearity, $K/W=11$. . .	65
21.	A Typical Control System.	14
22.	Solution of Sample Problem, First Multiple Nonlinearity .	66
23.	Sample Problem Containing Second Multiple Nonlinearity. .	19

LIST OF ILLUSTRATIONS (continued)

FIGURE		Page
24.	20 Log I/δ Versus $\sin^{-1}\delta/I$	67
25.	Solution of Sample Problem, Second Multiple Nonlinearity	68
26.	A Control System Containing Single Valued Nonlinearity .	27
27.	A Control System Containing Multiple Nonlinearity. . . .	29
28.	A Flow Chart Indicating the Computation of DIDF	33
29.	Block Diagram of the Sample Problem Containing the First Multiple Nonlinearity.	80
30.	Analog Computer Simulation of Problem Shown in Figure 29	81
31.	Block Diagram of the Sample Problem Containing the Second Multiple Nonlinearity	82
32.	Analog Computer Simulation of Problem Shown in Figure 31	83

ABSTRACT

Frequency response techniques are very valuable tools for the analysis and synthesis of linear control systems. To extend these techniques to the analysis of a nonlinear control system, it is necessary that the nonlinearity be described by an equation in the frequency domain and it also requires that this equation be compatible for use with the transfer functions of the linear components. This final report deals in general with the analysis of nonlinear control systems by describing function techniques and in particular with the derivation of the describing functions for the multiple nonlinearities that are often encountered in practice. The describing functions which are both amplitude and frequency dependent are associated with the multiple nonlinearities in which there are one or more energy-storage units together with a nonlinear characteristic which is related to the energy-storage property in such a way that a mathematical separation into distinct linear and nonlinear parts is not feasible. Therefore, for multiple nonlinearities a family of describing functions has to be generated. Such families of describing functions are generated for two multiple nonlinearities; (1) a deadzone followed by a first order linear block and backlash, and (2) a hysteresis relay followed by a second order linear block and backlash. Furthermore the generated data are presented in their most useful form (Nichols plots as well as tables).

The technique outlined in this report for obtaining the describing functions can be used in computing the describing functions for any other nonlinear combinations. A special method has been developed to take care of the amplitude dependency of the describing function family of the multiple nonlinearity containing a hysteresis relay. A number of methods

to find the transient response and the closed loop frequency response from the describing function data are outlined. A few sample problems are also presented indicating the use of the derived describing functions and the results are compared with the actual analog computer simulations of these problems.

CHAPTER I

INTRODUCTION

The Nyquist, Bode and Root locus techniques which form the basis of feedback system analysis are limited in applicability to linear systems. Methods available for analysis of nonlinear systems are not nearly as plentiful and as general in application as those developed for linear systems. Frequency response techniques are very valuable tools for the analysis and synthesis of linear systems. Part of the value lies in the simplicity of the block diagram and the transfer function representation and manipulation while the other part of the value lies in the ease of computation and interpretation using Bode diagrams and the Nichols plots. The difficulties encountered in nonlinear analysis are related to the exceedingly complex behavior of nonlinear systems as compared with the linear systems. For example, the response of a linear system is linearly dependent on the amplitude of the excitation; increasing the amplitude merely increases the amplitude of the output by the same multiple. With nonlinear systems, the output can be significantly dependent on the level or amplitude of excitation. Furthermore, if a linear system is excited by a sinusoidal forcing function, the output will be a sinusoid of different amplitude and phase but having the same frequency. The output of a nonlinear system forced in a similar manner may contain harmonics of the excitation frequency. It is desirable that the powerful methods of frequency response techniques be extended in such a way that they will be applicable to analysis and systhesis of nonlinear control systems.

Representation of nonlinear systems in a block diagram form is not very difficult. However, the nonlinear blocks impose a few restrictions

on the manipulation of the block diagram. The extension of the transfer function representation is more difficult; it requires that the nonlinearity be described by an equation in the frequency domain, and it also requires that this equation be compatable for use with the transfer functions of the linear components. This report deals in general with the analysis of nonlinear control systems by describing function techniques, and in particular with the derivation of the describing function for the multiple nonlinearities that are often encountered in practice. A discussion of all known frequency response techniques applicable to the describing function method is given. A few sample problems are presented which indicate the use of the derived describing functions. The results of these sample problems are compared with the results obtained from the actual analog computer simulations of these problems.

CHAPTER II

DESCRIBING FUNCTION METHODS

Since the very first publication of the paper concerning the describing function technique by R. J. Kochenbruger[1], many articles[2-18] have appeared in different journals and books on this subject. The describing function method is classified as a frequency response method rather than a time domain approach. It is based on an analysis which neglects the harmonic effects in the system. The basic idea involved in analyzing a nonlinear control system by this method is to replace the nonlinearity in the system by its describing function and use any suitable linear frequency response technique to analyze the system.

2.1 Definition: The describing function is defined as the ratio of the complex number representing the fundamental sinusoidal component of the output of the nonlinearity to the complex number representing the sinusoidal input.

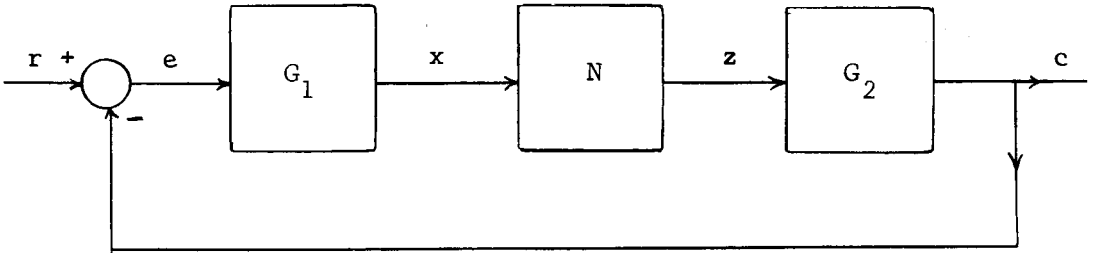

Figure 1 - A Control System

In terms of the elements shown in Figure 1, the describing function is defined as

$$G_D = \frac{Z_1(j\omega)}{X(j\omega)} \qquad (1)$$

where G_D is the describing function, $Z_1(j\omega)$ represents the fundamental component of the output $Z(j\omega)$ determined by the Fourier analysis and $X(j\omega)$ represents the sinusoidal input signal $x = X \sin \omega t$.

G_D may be a function of frequency as well as the amplitude of the input to the nonlinearity. If no energy storage elements are present in the nonlinearity 'N', then G_D is a function of the amplitude X alone. As can be seen, the replacement of the nonlinearity in a control system by its describing function is valid as long as the input to the nonlinearity is very nearly sinusoidal. The assumption which is usually made to justify[1-6] replacing the nonlinearity by its describing function is that the linear elements in a control system severely attenuate the higher harmonics generated by the nonlinearity and that only the fundamental component appears at the input of the nonlinearity. This assumption is often unnecessary depending upon the extent to which higher harmonics appearing at the input to the nonlinearity affect the amplitude and phase of the describing function. Now, consider the meaning of the describing function in a little more detail. When a nonlinearity is replaced by its describing function, a single sine wave of fundamental frequency is made to represent the nonsinusoidal output of the nonlinear element driven sinusoidally. This single sine wave is chosen as best in some sense. When a Fourier analysis is applied to obtain the best sine wave from the nonsinusoidal output of the nonlinearity, then the result is the best in a minimum-rms-error sense. It is possible to define many other forms of unconventional describing functions. An example can be given as to obtain a sine wave from the nonsinusoidal output of the nonlinearity in such a way that it will reduce the average error or the difference between the area of the selected sine wave and the actual output of the nonlinearity be zero. Another example of selecting the best sine wave may be such that a sine wave has

the amplitude equal to the peak value of the amplitude found in the non-sinusoidal output of the nonlinearity. But these unconventional describing functions do not appear to be of general usefulness. In fact, when the linear elements of the closed loop system tends toward a perfect low pass filter, the error of the conventional describing function tends toward zero.

A new RMS describing function[19] has been defined on an equivalent energy basis for single valued nonlinearities. The definition in terms of Figure 1 is,

$$\text{RMS Describing Function} = \left[\frac{\frac{1}{2\pi} \int_0^{2\pi} Z^2 \, d\omega t}{\frac{1}{2\pi} \int_0^{2\pi} (X^2 \sin^2 \omega t) \, d\omega t} \right]^{1/2}$$

Experimental evidence cited in the reference (19) indicates that the new RMS describing function gives more accurate results in a number of systems than does the conventional describing function. Since the new RMS describing function is prohibitively difficult to evaluate and use for multivalued nonlinearities, it is not employed for general use.

2.2 Stability Analysis: When the block diagram of any control system has been reduced to a single loop containing a nonlinear block as shown in Figure 1, the $\frac{C}{R}$ relationship can be written as

$$\frac{C}{R} = \frac{G_1(j\omega)\, G_2(j\omega)\, G_D}{1 + G_1(j\omega)\, G_2(j\omega)\, G_D} \qquad (2)$$

Let $G(j\omega) = G_1(j\omega)\, G_2(j\omega)$

The stability of the system is determined from the characteristic equation

$$G(j\omega)\, G_D = -1 \qquad (3)$$

The describing function, G_D, may in general be a function of amplitude and frequency of the sinusoidal excitation. Many times nonlinear control systems exhibit constant amplitude and constant frequency oscillations. These oscillations are called limit cycles. The occurence of limit cycles in the nonlinear systems makes it necessary to define instability in terms of the acceptable magnitudes of oscillations, since a very small nonlinear oscillation may not be detrimental to the performance of a system. On the contrary, sometimes such oscillation may even improve the performance of a system containing stiction or backlash. The limit cycles are called soft self-excited when they occur even in the presence of a very small input signal to the system. When the limit cycles occur only in the presence of very large input-signals, then they are called hard self-excited limit cycles.

Consideration of Equation (3) and the nature of G_D and $G(j\omega)$ shows that the self-sustained oscillations may exist when Equation (3) is satisfied, or when

$$G(j\omega) = -\frac{1}{G_D} \tag{4}$$

For a particular system, the functions $G(j\omega)$ and $-\frac{1}{G_D}$ can be sketched in the complex plane. The intersection between the loci of $G(j\omega)$ and $-\frac{1}{G_D}$ corresponds to the solution of the characteristic Equation (3). It thus represents a possible periodic solution to the equations describing the system.

If the nonlinearity in a system is such that its describing function is not a function of frequency and does not introduce any phase shift, then the describing function may be considered as a variable gain. The control system containing such a nonlinearity is stable if it is stable for the maximum gain. Single valued nonlinearities are of this type.

When such nonlinearities are present in conditionally stable systems, root locus and Bode plots are probably the simplest to use, since a variable gain introduces no change in any of the curve shapes.

Describing functions which are both amplitude and frequency sensitive are associated with components in which there are one or more energy storage units together with a nonlinear characteristic which is related to the energy-storage property in such a way that mathematical separation into distinct linear and nonlinear parts is not feasible. For such devices a family of describing functions has to be generated and a digital or analog computer may be necessary. For the stability interpretations of the control system containing nonlinearities whose describing functions are both amplitude and frequency sensitive, Nichols charts may be the most convenient to use. Chapter IV of this dissertation clearly outlines the use of Nichols charts in such cases.

When the intersection between $G(j\omega)$ and $-\frac{1}{G_D}$ has been determined or when the solution of the characteristic Equation (3) has been found, it is necessary to examine such a solution by perturbation techniques[18] to determine whether it represents a convergent equilibrium or a divergent equilibrium point.

CHAPTER III

THE DERIVATION OF THE DESCRIBING FUNCTIONS FOR TWO MULTIPLE NONLINEARITIES

Describing functions for a single nonlinearity have been derived by many authors[1-11] in the past. Describing function analysis has been successfully applied to control systems containing two nonlinearities which are adjacent in the control system.[12-15] In such cases a describing function of two nonlinearities is generated by considering them as a single nonlinear element. Sridhar[7] has suggested a general method for deriving describing function for a certain class of nonlinearities. By this method it is often possible to derive the describing function of two adjacent nonlinearities.

When two nonlinearities are separated by one or more linear blocks, the analysis becomes more complicated due to the fact that the input to the second nonlinearity depends upon the first in a manner such that it involves frequency. When the intervening linear block is of high order, it will act as a good low pass filter and the input to the second nonlinearity can be assumed sinusoidal. In such a case the analysis, even though a bit more complicated, can be carried out by techniques described by Thaler and Pastel.[6]

3.1 First Multiple Nonlinearity: Consider the problem of deriving the describing function of two nonlinearities separated by a first order linear block. Since the linear element contains insufficient filtering to permit the assumption of a sinusoidal input to the second nonlinearity the describing function has to be derived by considering the nonlinearities and the first order linear block as one nonlinear element. Such a describing function is amplitude and frequency dependent. A combination of

a deadzone with the half width as 'δ' and the backlash element with the width 'W' separated by a linear block $H(s) = \frac{K}{1 + \tau s}$ is shown in Figure 2.

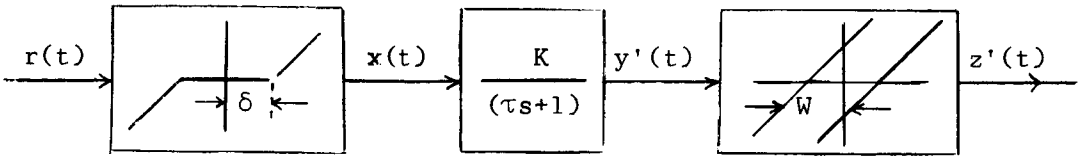

Figure 2 - First Multiple Nonlinearity

Actually Figure 2 can be redrawn as follows.

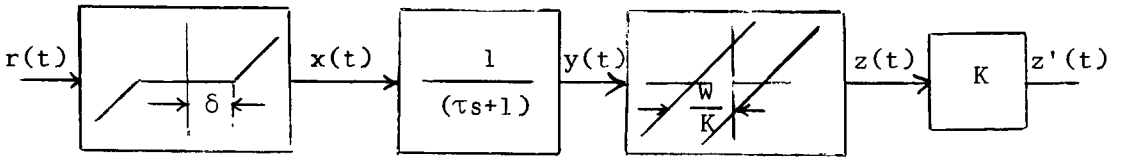

Figure 3 - Nonlinearity Equivalent to First Multiple Nonlinearity

If the nonlinearity of Figure 2 is a part of the closed loop system as shown in Figure 1, then it can be replaced by Figure 3 and the gain K can be combined with the linear block. So it is only necessary to derive the describing function for Figure 3. The response x(t) of the deadzone to a sinusoidal input function $r = I \sin \omega_o t$ is indicated in Figure 4.

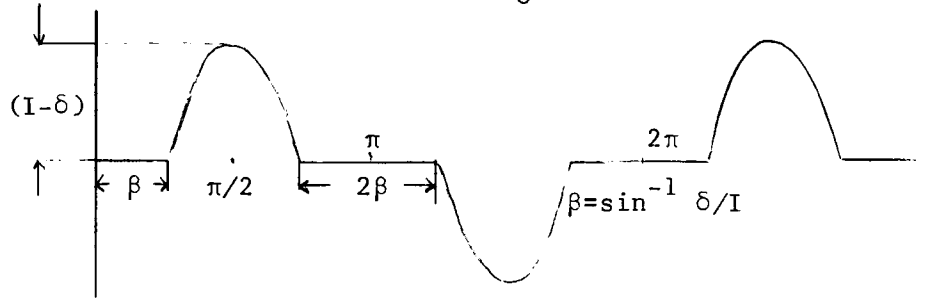

Figure 4 - Output of the Deadzone Element

In terms of the elements given in Figure 3 and Figure 4, x(t) can be written as

$$\begin{aligned} x(t) &= 0 && 0 \leq \omega_o t \leq \beta \\ &= (I \sin \omega_o t - \delta) && \beta \leq \omega_o t \leq \pi - \beta \\ &= 0 && \pi - \beta \leq \omega_o t \leq \pi + \beta \\ &= (I \sin \omega_o t + \delta) && \pi + \beta \leq \omega_o t \; 2\pi - \beta \\ &= 0 && 2\pi - \beta \leq \omega_o t \leq 2\pi \quad - - - \end{aligned} \tag{5}$$

To compute y(t), let H(s) be subjected to a periodic function x(t). Define $x_1(t)$ such that it equals x(t) for only one cycle or

$$x_1(t) = x(t) \; - - - \; 0 \leq \omega_o t \leq 2\pi$$

$$= 0 \; - - - \; \omega_o t > 2\pi$$

Then $x(t) = \sum_{K=0}^{\infty} x_1\left(t - \frac{2\pi K}{\omega_o}\right) u\left(t - \frac{2\pi K}{\omega_o}\right)$ where u is a unit step function.

The Laplace transform of $x(t) = X(s) = X_1(s) \sum_{K=0}^{\infty} e^{-\frac{2\pi K}{\omega_o} s}$

The complete response for all time is therefore,

$$y_c(t) = \mathcal{L}^{-1} X(s) H(s)$$

$$= \mathcal{L}^{-1} \frac{X_1(s) H(s)}{(1 - e^{-2\pi s/\omega_o})} \quad - - - - - - - \tag{6}$$

In evaluating the complete response $y_c(t)$ for all time the residue of $Y_c(s)e^{st}$ at the singular points of X(s) constitute the steady state response and those at the singular points of H(s) constitute the transient.[16] This transient solution can therefore be written as

$$Y_T(t) = \sum \text{Residue of } \frac{X_1(s) H(s) e^{st}}{(1 - e^{-2\pi s/\omega_o})} \text{ at the poles of H(s)} \tag{7}$$

Subtracting the transient response from the complete solution for the first period, the result will be the steady state solution y(t).

$$y(t) = y_c(t) - y_T(t) = \mathcal{L}^{-1} X_1(s)H(s) - y_T(t) \text{ - - - } o \leq \omega_o t \leq 2\pi \text{ ---(8)}$$

As shown in Appendix I, y(t) can be derived by a consideration of Equations (5), (6), (7), and (8). The steady state output z(t) of the backlash element can be determined from y(t). Let the maximum of y(t) = M and suppose this maximum occurs at $t = T_M$. Then for $M > W$

$$z(t) = y(t) - W/2 \text{ - - - } o \leq t \leq T_M$$

$$= y(T_M) - W/2 \text{ - - - } T_M \leq t \leq T_B$$

$$= y(t) + W/2 \text{ - - - } T_B \leq t \leq \pi/\omega_o$$

where T_B is defined by $W = \left| y(T_B) - y(T_M) \right|$. For $W/2 \leq M \leq W$

$$z(t) = -(M - W/2) \text{ - - - - } o \leq t \leq T_c$$

$$= y(t) - W/2 \text{ - - - - - - } T_c \leq t \leq T_M$$

$$= M - W/2 \text{ - - - - - - } T_M \leq t \leq \pi/\omega_o$$

where T_c is defined by $y(T_c) = W - M$. The describing function can then be determined as indicated in Appendix II. For values of $\tau\omega_o \ll 1$, the two nonlinearities can be considered as one nonlinear element and its describing function is derived in Appendix III. The values of G_D and ϕ for various values of nondimensionalized frequency $\tau\omega_o$, normalized ratio $\delta K/\omega$ and δ/I are listed in Tables I through VII. Since the intent is to present the data in such a way that it can be conveniently used, Nichols plots of the describing function are given in Figure 5 through Figure 11.

3.2 Second Multiple Nonlinearity: Another problem of interest is that of two nonlinearities separated by a second order linear block which is underdamped. A nonlinear block of relay with hysteresis, second order linear block and backlash is shown in Figure 12.

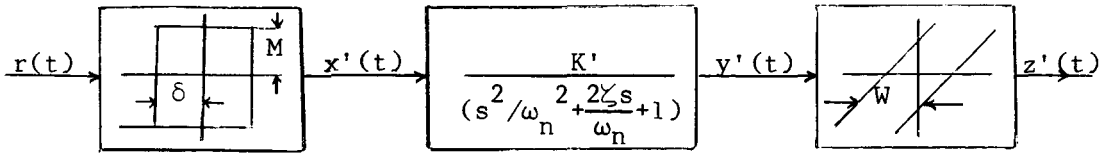

Figure 12 - Second Multiple Nonlinearity.

The input to the second nonlinearity, that is backlash, can be rich in harmonics when the nonlinear block is driven with a sinusoid. The harmonic content will of course be a function of input sinusoidal frequency, zeta and ω_n. Therefore, the describing function has to be derived by considering the nonlinearities and the second order linear block as one nonlinear element. Figure 13 is functionally equivalent to Figure 12. Therefore, the describing function for Figure 13 will be derived. Let MK' = K.

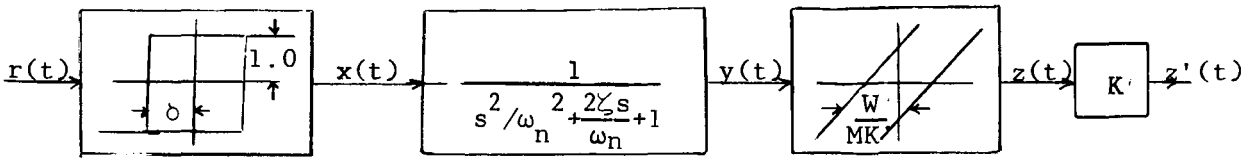

Figure 13 - Nonlinearity, Equivalent to Second Multiple Nonlinearity

The response x(t) of the relay with hysteresis, to a sinusoidal input function r = I sin $\omega_o t$ is shown in Figure 14.

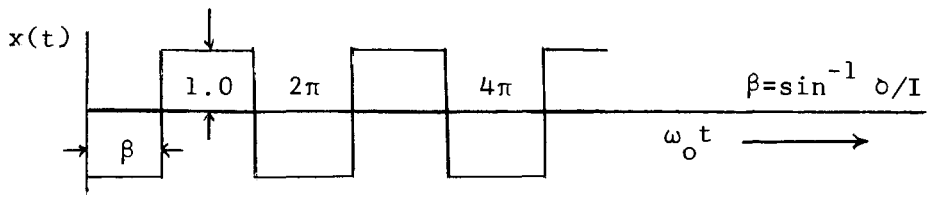

Figure 14 - Output of the Relay with Hysteresis.

From a consideration of Figure 14, it can be seen that x(t) is always a square wave with a unity amplitude and its frequency is equal to that of the input excitation. Only the phase shift changes with the magnitude of I. Therefore, for all practical purposes the second order linear block has an input of a square wave with the fixed amplitude of unity and frequency equal to ω_o. The first step is, therefore, to derive the output y(t) of the second order linear block when excited with a square wave. From y(t), z(t) can be computed exactly in the same manner as the previous nonlinearity and then the fundamental Fourier Component A_1 and B_1 of z(t) can be obtained by numerical techniques. The details of the computation of y(t) are shown in Appendix IV, while the computation of z(t) and the fundamental Fourier components A_1 and B_1 are indicated in Appendix V. When $\omega_o/\omega_n \ll 1.0$, the nonlinearities can be considered as being adjacent to each other and its describing function is derived in Appendix VI. Note that G_D is computed for $\delta = 0.0$ and I = 1.0, since for a given δ the phase shift of $\sin^{-1} \delta/I$ for various values of I can be added to the describing function and its magnitude can be divided by the value of I later on. The values of the describing function G_D and phase ϕ for various values of the nondimensionalized frequency ω_o/ω_n, normalized ratio K/W and zeta are listed in Table VIII through Table XIII. Again the intent being to present the data in its most useable form, the Nichols plots of the describing functions are given in Figure 15 through Figure 20. The use of these plots are a little complicated but once the technique is understood by the user it is quite straightforward.

CHAPTER IV

SAMPLE PROBLEMS INDICATING USE OF THE GENERATED DESCRIBING FUNCTIONS

The describing functions for two multiple nonlinearities have been derived in the last chapter and the Nichols Plots of these describing functions are given in Figure 5 through Figure 11 and Figure 15 through Figure 20. In using these plots there are several variables which allow the engineer a great deal of flexibility in desiging for the proper control system performance. A typical control system is shown in Figure 21 where $G_L(j\omega_o)$ is any linear plant transfer function and G_D is the describing function of the combined nonlinear block.

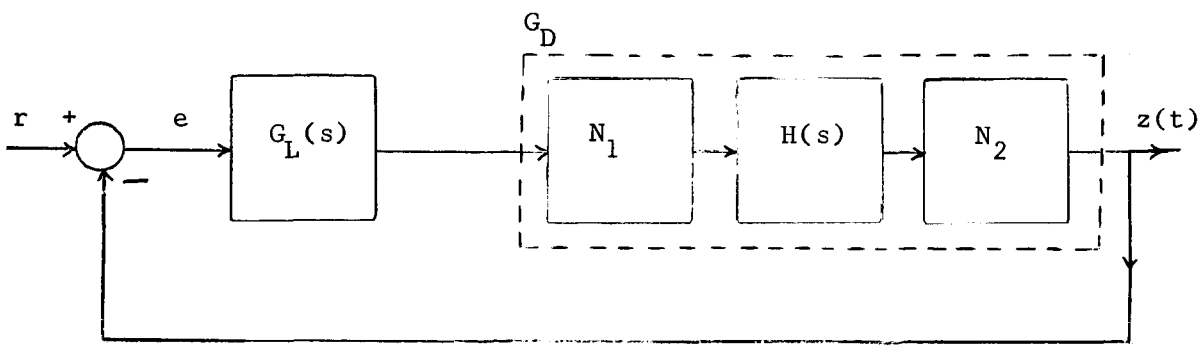

Figure 21 - A Typical Control System

In using the describing function curves, several points must be considered:

(1) The problem parameters that are fixed and that are variable;

(2) Whether all limit cycles are to be avoided as undesirable;

(3) The distribution of gain between the linear and the nonlinear block.

4.1 A Sample Problem Containing First Multiple Nonlinearity: Consider a

control system in which the nonlinear block consists of a deadzone, backlash and a separating linear block. Since for the stability analysis the characteristic equation

$$G_L(j\omega_o)\, G_D(I,\omega_o) = -1$$

has to be solved, the following steps indicate the procedure.

(1) Form a $\delta K/W$ ratio and select the corresponding describing function family of Nichols plot from Figure 5 through Figure 11.

(2) Plot $K\,|G_L|$ versus its phase angle θ_L with $\tau\omega_o$ as a parameter.

(3) Superimpose the curve plotted in step (2) on the describing function family selected in step (1) and look for an intersection between these curves at a proper value of $\tau\omega_o$. If the intersection exists, then it can be a convergent or a divergent equilibrium point and a stable or an unstable limit cycle may exist. Consider a specific problem in which

$$G_L(j\omega_o) = \frac{5}{j\omega_o(j\omega_o + 1)} \quad ,$$

$$K = 1.0 \ ,$$

$$\delta = W = 1.5 \text{ units} \ ,$$

and $$\tau = 0.1$$

The plot of $|G_L|$ versus θ_L with $0.1\ \omega_o$ as the parameter is shown in Figure 22. As $\delta K/W = 1.0$, Figure 5 is the appropriate describing function family. Superimposing $|G_L|$ versus θ_L plot on Figure 5 indicates that the intersection occurs at $\omega_o = 1.25$ radians/seconds. Further examination by perturbation technique[18] reveals that this intersection is a convergent equilibrium point and the system will have a stable limit cycle. The limit cycle amplitude can be read off the curves if this information is desired. The intersection point is on the curve $\delta/I = 0.41$.

Since $\delta = 1.5$, $I = \frac{1.5}{0.41} = 3.56$. There are many more variations to this example which can be presented. For instance 'K' can be varied which in turn changes the important $\delta K/W$ parameter. The time constant τ can also be varied.

It should be noted that if no intersection between $|G_L|$ versus θ_L curve and the appropriate describing function family exists, it does not necessarily mean that the system is stable. On the contrary such a system may be completely unstable for it may possess negative phase margin. This can be determined as follows. Suppose the system is completely unstable. Then the amplitude 'I' will continusously increase in time and will become appreciably larger than δ and W. In such cases the appropriate describing function family of Nichols plot will be reduced to a single curve corresponding to $\delta/I = 0.0$. If we can locate a frequency on $|G_L|$ versus θ_L curve such that the gain in dbs at this frequency is identical to the corresponding frequency on the curve reduced from the describing function family of Nichols plot for $\delta/I = 0.0$, then the system is completely unstable; otherwise it is stable.

4.2 A Sample Problem Containing Second Multiple Nonlinearity: When a control system contains a relay with hysteresis followed by a second order linear block and backlash, the stability analysis is similar to that discussed earlier in this chapter; but the procedure of investigating the existence of limit cycles is altogether different. The describing function for the second multiple nonlinearity was derived for a particular case in which δ, the half hysteresis width of the relay, was considered zero and the input sinusoidal excitation to the relay had a fixed amplitude of 1.0.

Since in a control problem, the relay hysteresis may not be zero and the amplitude of the limit cycle may be other than 1.0, the derived des-

cribing function curves have to be used with some care. Note that the describing function was defined (refer to Figure 13 and Appendix V) as

$$|G_D| = \frac{\sqrt{A_1^2 + B_1^2}}{I} \qquad (9)$$

where A_1 and B_1 are the fundamental Fourier components of z(t). Equation (9) can be written as

$$G_D = \frac{\sqrt{A_1^2 + B_1^2}}{(1/(\delta/I))} \cdot \frac{1}{\delta}$$

$$\therefore \quad 20 \log \left[\frac{1}{|G_D|}\right] = 20 \log \frac{1/\delta/I}{\sqrt{A_1^2 + B_1^2}} + 20 \log \delta$$

$$= 20 \log \frac{1}{\sqrt{A_1^2 + B_1^2}} + 20 \log \left[1/(\delta/I)\right] + 20 \log \delta.$$

It was also observed that the relay hysteresis merely produces a phase shift in its output when excited with a sinusoid, and the output wave shape is unaltered eventhough the amplitude of the sinusoidal excitation is varied. So, for a general problem, among the parameters in the derived describing function curves, the phase shift has to be modified by $\sin^{-1} \delta/I$ and the magnitude by $\left[20 \log (1/\delta/I) + 20 \log \delta\right]$. Note that 'I' can never be less than δ and for $\delta = I$, $\sin^{-1} \delta/I = 90$ degrees. The procedure of modifying and using the derived describing function curves for a general problem is as follows.

(1) For a certain problem zeta, ω_n, K, δ and W are given. Also the linear block transfer function G_L is given. Plot $K|G_L|$ versus its phase angle θ_L with ω_o/ω_n as the nondimensionalized frequency.

(2) Find 20 log δ

(3) Select the proper describing function curve for appropriate K/W and zeta, from Figure 15 through Figure 20.

(4) Overlay the describing function curve obtained in step (3) on the plot of $K|G_L|$ versus θ_L obtained in step (1), coinciding the (0db, -180°) point of the describing function curve with the (0db, -90°) point of the plot of $K|G_L|$ versus θ_L.

(5) Move the describing function graph directly upwards by the dbs obtained in step (2).

(6) Obtain a curve of 20 log (I/ò) vs $\sin^{-1}$ (ò/I) with the ratio of ò/I as running parameter. Note that this is a generalized curve and should be kept with the describing function plots for any future use. Such a curve is shown in Figure 24.

(7) Superimpose the curve of Figure 24 on the describing function curve by coinciding ò/I = 1.0 point at any frequency on the describing function curve. If the curve of Figure 24 intersects the plot of $K|G_L|$ versus θ_L at the same frequency then we have a limit cycle at that frequency. The amplitude of the limit cycle can be determined from the value of ò/I at which Figure 24 intersects with the plot of $K\backslash G_L\backslash$ versus θ_L.

Consider a sample problem shown in Figure 23. The plot of $K|G_L|$ is shown in Figure 25. Since K/W = 1.0 and zeta = 0.1, the proper describing function curve is Figure 15.

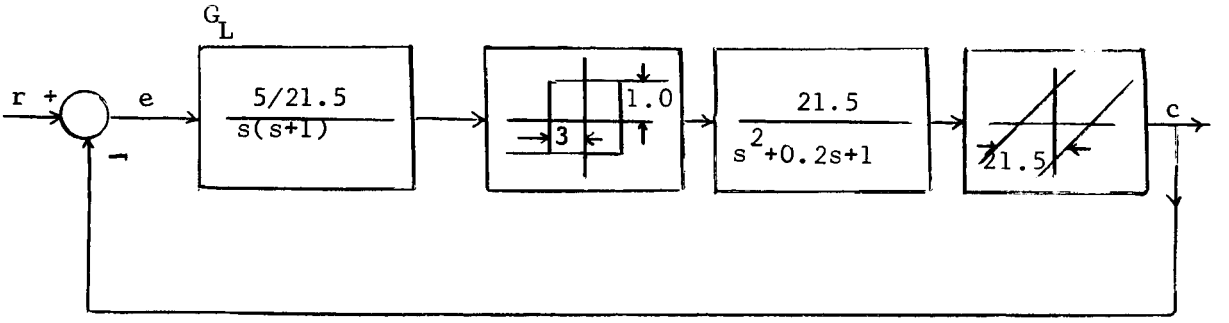

Figure 23 - A Sample Problem Containing Second Multiple Nonlinearity.

Now 20 log δ = 20 log 3.0 = 9.542; therefore superimpose the describing function of Figure 15 on Figure 25 such that the zero db axis is exactly 9.542 dbs above, and -180° point on the describing function curve coincides with -90° point of the plot of K $|G_L|$ versus θ_L curve. Superimpose Figure 24 on the describing function curve such that δ/I = 1.0 point coincides with frequency ω_o/ω_n = 0.823. The curve of Figure 24 will intersect K $|G_L|$ versus θ_L curve at ω_o/ω_n = 0.823 and δ/I = 0.2. So the limit cycle frequency is 0.823 radians/seconds and the amplitude I = δ/0.20 = 3/0.20 = 15.0 units.

It is interesting to note that for values of δ approaching zero, the quantity 20 log δ is going to approach minus infinity. According to the step (5), the selected describing function plot will have to be moved to minus infinity and then Figure 24 will be used to find the appropriate intersection with the K $|G_L|$ versus θ_L curve. As a matter of fact when δ = 0, there is a simpler procedure to solve the problem since the describing function plots shown in Figure 15 through Figure 20 are derived for δ = 0.0 and I = 1.0. In such a case simply overlay the describing function curve obtained in step (3) on the plot of K $|G_L|$ versus θ_L

obtained in step (1), coinciding the (0db, -180°) points of both the curves with each other. Move the describing function curve directly up or down and locate the intersection between the describing function plot and $K|G_L|$ versus θ_L plot at a common frequency. This will be the limit cycle frequency. The amplitude of the limit cycle can be found from the amount of displacement of the describing function plot since it will be equal to 20 log I.

In practice, many control systems have more than one nonlinear relationship in the control sequence. Some practical cases in which the two multiple nonlinearities discussed in this dissertation are present include:

(a) A simple relay servomechanism in which a relay with hysteresis drives a torque motor, the output shaft of which has a free play.

(b) Systems containing two stages of pneumatic amplification, the first stage amplifier having a deadzone while the second stage has a first order lag and it drives a gear train which has a backlash.

(c) A gyroscope measuring the difference between the desired roll angle and the actual roll angle having a deadzone, actuates a servomechanism having a first order lag which in turn actuates the ailerons which has a free play.

(d) A time optimum control system in which an on-off device drives an underdamped second order servo, the mechanical output of which has a backlash.

CHAPTER V

ACCURACY CONSIDERATIONS AND COMPARISON WITH ANALOG COMPUTER RESULTS

The describing function is derived under the assumption that the input signal to the nonlinearity element is sinusoidal. It follows that the describing function will provide accurate results when this basic assumption is satisfied. Admittedly the describing function method is an approximate one since the results are less accurate when the harmonics in the input signal to the nonlinearity are not negligible. There is no way to compute *a* universal 'corrected' describing function since the error depends on the filtering action of the linear system in which the nonlinearity is incorporated. A knowledge of the harmonic content in the output of the nonlinearity when subjected to a sinusoidal input, provides an indication of the possible difficulties and this must be compared with the filtering capabilities of the linear system.

In the analysis of nonlinear control system by describing function methods, intersections between the locus of $|G_L|$ versus θ_L and the appropriate family of Nichols plots, define stable or unstable limit cycles and the interpretation is simple and accurate. However, difficulty sometime arises owing to intersections which should not exist and which predict limit cycles that do not occur in the physical system. Another difficulty arises if a limit cycle that has not been predicted because the loci are quite close but do not actually intersect, appears in the physical system. These discrepancies between the predicted and observed limit cycles are obviously due to the neglect of circulating harmonics in the system. Fortunately most servo systems contain linear elements which act as effective low pass filters. Consequently, eventhough the output of the nonlinear ele-

ment be rich in harmonics, in a complete trip around the loop the harmonics may be so attenuated that the input to the nonlinear element is again nearly sinusoidal. This discrimination against higher harmonics tends to increase with the complexity or order of the system. In this lies one of the great attractions of the method since it means that more complicated systems for which conventional methods might be completely impractical are most effectively and simply handled by describing function method.

E. C. Johnson[2] has suggested a method to evaluate the correction terms which correct both amplitude and frequency of the limit cycle as predicted by the describing function method. The derivation is limited to single valued differentiable nonlinear functions, eventhough Johnson has applied the correction terms to a nonlinearity which does not meet the requirements stated above. Essentially this method consists of expressing the amplitude and frequency of the limit cycle in two separate power series of a perturbation parameter μ. When μ is zero both the series reduce to the solutions obtained from the conventional describing function, and when $\mu=1$ the series represent the correct solutions. The evaluation of the coefficients of the power series is very complex and in the main this analysis simply serves to give better feeling for the relative accuracy of the describing functions. Since the generated describing functions in this dissertation are amplitude and frequency sensitive, the accuracy of the results for the sample problems was checked from the actual analog computer simulation of the problems. The details of the analog computer simulation and the comparison of the analog results with the theoretical predictions are shown in Appendix VII and Appendix VIII.

CHAPTER VI

TRANSIENT RESPONSE AND CLOSED LOOP FREQUENCY RESPONSE FROM DESCRIBING FUNCTION DATA

The primary functions of describing function analysis and design are to check stability of a nonlinear system and to design a compensation which provides a stable system. Prediction of the step response and the closed loop frequency response of the nonlinear systems is also desired. Some attempts have been made to predict the closed loop frequency response and transient response characteristics of nonlinear control systems by applying linear-frequency-response correlation techniques in conjunction with the describing function.

6.1 Transient Response: For a nonlinear system, the principle of superposition is not valid and therefore the correlations between the frequency response and transient response which are developed for linear systems are not strictly applicable to nonlinear systems. By replacing the nonlinearity with its describing function, the control system is essentially linearized and therefore the transient performance of the linearized system may be estimated. But this estimate is not accurate as is the case with linear systems. For a complete system design, it is necessary that a satisfactory transient response be obtained. Quantitative predictions of the transient response are desired but for a linearized nonlinear system only qualitative predictions are possible which are also useful.

Finnigan Approach: Finnigan[21] has suggested a method of computing an approximate transient response of a nonlinear system to a step function with the aid of root-locus. The particular nonlinearity considered in his work is that of backlash. The method starts with the modification of linear

root locus by the describing function. When the describing function does not introduce a phase shift, the root points for the various amplitude input signals to the nonlinearity are computed and marked on the linear-system root locus. The root locus itself has to be modified using the phase angle and gain when the describing functions introduce a phase angle. It is noted that for a lightly dampened system, the transient oscillations are nearly sinusoidal and any half cycle may be approximated fairly accurately as a sine wave. The selection of the amplitudes of the approximating sine wave is carried out as follows. First the system is assumed linear and the percent overshoot for a specified step input is determined. The peak displacement is then computed and this value is used as an approximation to the peak to peak amplitude of the first segment. Since the amplitude of the input to the nonlinearity is known, the roots are immediately located and with these roots the peak overshoot is again determined and the process is thus continued. When a describing function of the nonlinearity does not introduce a phase shift, the application and interpretation of the results using this method is not difficult. But when the describing function of the nonlinearity introduces a phase shift, another complication arises with the fact that the root locus on the real axis of the linear system is converted to a locus with the complex values. Even if an assumption of symmetrical root locus along the real axis is made, it is hard to interprete physically by virtue of the fact that a real root is suddenly replaced by a complex pair of roots. The extension of this method to the describing function which are frequency and amplitude sensitive appears to be almost impossible.

Kochenburger Approach: Another method for a qualitative correlation is suggested by R. J. Kochenburger[1] for relay servos. The first step in this

method is to plot the Nichols plots of the describing function of the nonlinearity similar to Figure 5 through Figure 11 and $|G_L|$ versus θ_L curve and establish that the system is stable. Since the Nichols plots of the describing function represents a locus of the critical points, the entire closed loop frequency response may be determined for each point by superimposing M and N contours centered at each critical point and reading off the M and N values at the intersection of these contours with the $|G_L|$ versus θ_L curve. The describing function considered by R. J. Kochenburger is amplitude dependent only. A specific point on the Nichols plots of the describing function represents a certain input amplitude of the sinusoid and a specific resonance peak M_m and the corresponding resonance frequency ω_m which can be determined by the point of tangency between the $|G_L|$ versus θ_L curve and some M contour. This procedure is repeated for several other points on the Nichols plots of the describing function and the plots of M_m and ω_m versus the amplitude of the sine wave are made. The general characteristics of the step response can now be deduced qualitatively from these curves. Such a deduction is postponed until a method for obtaining such curves for the multiple nonlinearity case is outlined.

When a control system contains either of the multiple nonlinearities presented in Chapter III, the stability analysis of the system is first carried out as indicated in Chapter IV. Note that for a specific control problem containing the multiple nonlinearities, Nichols plots of the describing function are a family of curves. In such a family of curves the points of constant (δ/I) are indicated (Figure 5 through Figure 11 and Figure 15 through Figure 20 along with Figure 24). Since δ is a known fixed quantity for a given problem, the constant (δ/I) points represent a certain amplitude I of the input sinusoid to the multiple nonlinearities.

The first step, therefore, is to select one constant (δ/I) line say (δ/I_1) from the family of describing function plot. At a point on this line superimpose constant M and N contours. Remember that this selected point corresponds to a certain frequency. Find the M contour which passes or touches the $|G_L|$ versus θ_L locus at the same frequency and note the frequency and M value. Repeat this process at several other points on the constant (δ/I_1) curve noting at each point the frequency and M value. Select the largest value of M amongst the recorded values and the corresponding value of the frequency and enter this in a table against I_1. Repeat the entire process for many other values of I, say (δ/I_2, δ/I_3 --) and note the corresponding maximum values of M and frequencies. Plot the recorded values of M_m and frequencies against the values of I. From these curves the general characteristics for the step response can be qualitatively deduced[1]. If M_m is small for large input signal amplitudes I, but large for small input signal amplitudes, then for a step input it is expected that the system will be well dampened with moderate peak overshoot; however as the amplitude of oscillations decreases, the system dampening decreases and the oscillations will persist with relatively slow decrement. If the resonant frequency is high for large input signals but decrease with decreasing amplitude signal, then the frequency of transient oscillations will decrease as the oscillations die out.

6.2 Closed Loop Frequency Response: Many authors[21-23,6,18] have presented various methods of finding closed loop frequency responses of nonlinear control systems. The procedure to find such a response invariably begins with the conventional describing function which is only am-

plitude sensitive and in some cases extension is suggested for the frequency sensitive describing functions.

Gibson's Approach: For a single-valued nonlinearity Gibson's[18] approach appears most practical and straightforward.

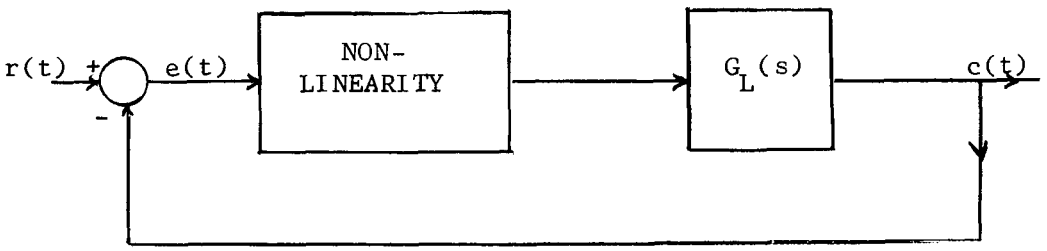

Figure 26 - A Control System Containing Single Valued Nonlinearity

In terms of Figure 26

$$\frac{e(j\omega_o)}{r(j\omega_o)} = \frac{1}{1 + G_D\, G_L(j\omega_o)} \qquad \text{- - - - - - - - - -} \quad (10)$$

Where G_D is the describing function of the single valued nonlinearity and let $r = R \sin \omega_o t$.

Assuming that the basic assumption of the describing function holds for this system, then $e = I \sin(\omega_o t + \phi)$. The magnitude relationship of Equation (10) would be

$$\frac{I}{R} = \left| \frac{1}{1 + G_D\, G_L(j\omega_o)} \right| \qquad (11)$$

Knowing the linear transfer function $G_L(s)$, it is possible to rearrange Equation (11) such that the left hand side of the equation will consist of only G_D.

Let $G_L(j\omega_o) = \alpha(\omega_o) + j\,\beta(\omega_o)$

then $$\frac{I}{R} = \left| \frac{1}{(1 + \alpha G_D) + j\,\beta\, G_D} \right|$$

$$\therefore \quad (\alpha^2 + \beta^2)\, G_D^{\,2} + 2\alpha\, G_D + (1 + R^2/I^2) = 0.0$$

or

$$G_D = -\frac{\alpha}{(\alpha^2 + \beta^2)} \pm \frac{1}{(\alpha^2 + \beta^2)} \sqrt{\alpha^2 - (\alpha^2 + \beta^2)(1 - R^2/I^2)} \qquad (12)$$

Note that while deriving Equation (12), use is made of the fact that G_D is real. Since G_D is a function of I, both sides of the Equation (12) can be plotted as a function of I with a fixed value of R and ω_o. The left hand side is a familiar describing function plotted as a function of the amplitude of the input sinusoids and needs to be plotted only once. The right hand side of Equation (12) has to be plotted for several values of ω_o but keeping R fixed throughout. The intersection of G_D locus with the locus of the right hand side of Equation (12) represents a steady operation point for each frequency. Now knowing the amplitude I and the frequency at the intersection point $|c|$ can be obtained, since $|c| = I \cdot G_D \cdot G_L(j\omega_o)$. The quantity $|c|$ versus frequency can then be plotted. This is the desired result. Sometime it is possible to find two stable intersections between G_D locus and the right hand side of Equation (12) versus I locus in a narrow band of frequencies. This is the so called jump phenomena, peculiar to nonlinear systems.

When the nonlinearities are nonsingle valued and the describing function of which may be a function of amplitude and frequency, Hill's[23] method or Thaler's[6] method for finding closed loop frequency response are convenient. There is essentially no difference between the two methods. Thaler's Method: For the system shown in Figure 27 the multiple nonlinearities may be either of the two for which the describing function is generated in this dissertation.

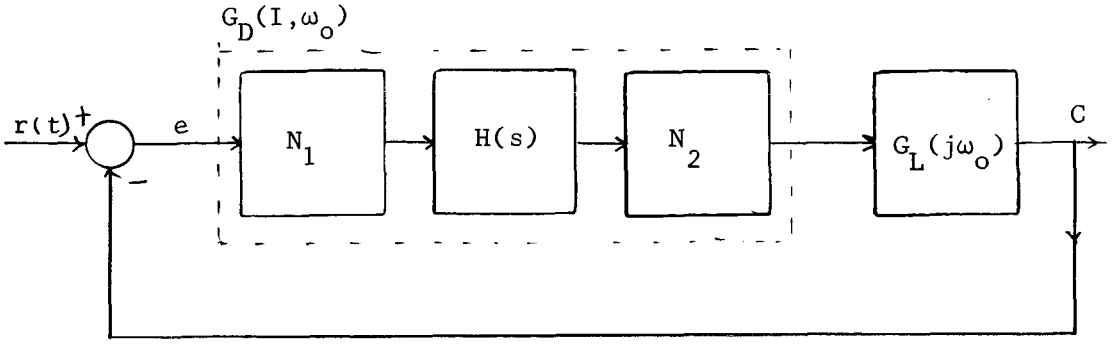

Figure 27 - A Control System Containing a Multiple Nonlinearity

Let $r = R \sin(\omega_o t)$ and assuming G_L being a low pass filter let $e = I \left[\sin(\omega_o t + \phi)\right]$. Now

$$\left| \frac{C(j\omega_o)}{R(j\omega_o)} \right| = \left| \frac{G_D\, G_L(j\omega_o)}{1+G_D\, G_L(j\omega_o)} \right| = M$$

Usually for a constant value of R and varying a ω_o, the $|c|$ versus ω_o curve is desired. The procedure used to determine the frequency response curve is similar to that followed in estimating the transient response qualitatively. For constant values of I, a family of M versus frequency and N versus frequency curves are generated. The Bode plot of the linear block $G_L(j\omega_o)$ is plotted and used as a nomograph. From such a Bode plot the value of $|G_L|$ db is found for any frequency. Since $|c(j\omega_o)| = I\,|G(j\omega_o)|\,|G_D(I,\omega_o)|$ for a falue of I and ω_o, $|c|$ can be determined. From the relationship $M = |c(j\omega_o)| / |R(j\omega_o)|$ the value of R is determined since the value of M for a frequency ω_o and I is already known. This value of R is marked on the M and N versus frequency curves. This process is continued for many other values of I and ω_o. The locus of all the points of a constant R is the desired frequency response curve.

Hill's Method: This method is based upon a functional transformation similar in philosophy to the Nichol's chart for linear systems. From a consideration of Figure 27 the following equations can be written. Let $r = R \sin \omega_o t$.

$$\frac{E(j\omega_o)}{R(j\omega_o)} = \frac{1}{1 + G_D(I,\omega_o)\, G_L(j\omega_o)}$$

or

$$|E| \angle \alpha(\omega_o) = \frac{1}{1 + |G_D| \angle \phi_D |G_L| \angle \gamma(\omega_o)} \quad |R| \angle o$$

$$= \frac{1}{1 + |G_D| \angle \phi_D |G_L| \angle \gamma(\omega_o)} \quad |R| \angle \psi(\omega_o) \qquad (13)$$

where

$$\psi(\omega_o) = \text{argument of } \left[\frac{1}{1 + G_D(I,\omega_o) G_L(j\omega_o)} \right]$$

Define

$$zdb = 20 \log_{10} \left| \frac{1}{1 + G_D(I,\omega_o) G_L(j\omega_o)} \right| .$$

Considering magnitudes of Equation 13 only the relation,

$$|E| \text{ db} = Zdb + Rdb \qquad (14)$$

can be written. The computational procedure begins by assuming a value of $|E|$ db. Since G_D is a function of $|E|$ db, zdb can be computed only when $|E|$ db is known. If Zdb and Rdb adds to the assumed value of $|E|$ db, then a solution to Equation 14 is indicated. The computation of Zdb from an assumed E db is accomplished from a chart for the functional transformation

$$F(\omega_o) \angle \theta(\omega_o) \text{ to } \frac{1}{1 + F(\omega_o) \angle \theta(\omega_o)}$$

This is similar in concept to the familiar Nichol's Chart. In fact, the required transformation, is accomplished by using a conventional Nichol's Chart, which is inverted. Such a chart is often called a Lohcin Chart. Again, the object is to find the closed loop frequency response of the system for a fixed amplitude of the input R and varying ω_o. The following steps indicate the procedure for finding such a response.

(1) For the given problem of Figure 27, select the appropriate Nichols family of $-\frac{1}{G_D}$ from Figure 5 through Figure 11 or Figure 15 through Figure 20.

(2) Plot $20 \log_{10} \left| G_L(j\omega_o) \right|$ versus phase angle of $G_L(j\omega_o)$ with frequency as a parameter and superimpose this curve on the Nichols family selected in step (1).

(3) If the family of plots selected in step (1) is from Figure 5 through Figure 11, then on such plots the lines of constant δ/I and $\tau\omega_o$ are indicated. For a given problem, δ and τ are known. So these lines represent constant I and constant ω_o lines. If the plot selected is from Figure 15 through Figure 20, then the superimposed curve of Figure 24 at a particular frequency, represents a constant frequency line. On Figure 24, the points of the ratio δ/I are indicated.

(4) Assume a value of I somewhere on a constant ω_o line on the Nichols family selected in step (1) and place the origin of the inverted Nichol's or Lohcin Chart on this point.

(5) At the same ω_o point on the curve plotted in step (2), read the value of Zdb from the overlay of the Lohcin Chart.

(6) Add the assumed Rdb to Zdb found in step (5). If this equals the assumed value of Idb in step (4), then a solution to

Equation 14 has been found. There may be several Idb solutions for the same ω_o line. If a solution is not obtained, select another Idb point and repeat the procedure.

(7) After finding a solution point as indicated in step (6), place the origin of the Nichol's Chart on this point and read the value of (C/R) db from the overlay corresponding to the frequency ω_o on the curve plotted in step (2). Add to this value of (C/R)db, the assumed value of Rdb. Thus the required value of Cdb is obtained. This is the desired closed loop response for the input $r = R \sin \omega_o t$.

The closed loop frequency response derived from the conventional describing function fails to indicate the possible existence of subharmonic oscillations and the stability of the forced oscillations. Dual input describing function (DIDF) is an attractive tool to determine the stability of forced oscillation, the possible existence of jump phenomena and subharmonic oscillations.

DIDF (Input Sinewaves Harmonically Related): The dual input describing functions is derived by the same procedure as the conventional describing function, with the exception that the nonlinearity has two sine waves at the input, one of the sine waves being a multiple or harmonic frequency of the other. That is,

$$x(t) = I \cos(\omega_o t + \phi) + \beta \cos n \omega_o t$$

The magnitude of the DIDF is defined as,

$$\left| \text{DIDF} \right| = \frac{\text{amplitude of desired frequency component in output}}{\text{amplitude of the same frequency component in input.}}$$

The phase shift of the DIDF is defined as the shift from input to output of the same frequency component. Since there are two components in the input, a describing function is defined for each. Each DIDF for any nonlinearity is a function of at least four parameters, I, β, ϕ and n. When the nonlinearity contains an energy storage element, then the DIDF is a function of ω_o, in addition to the four parameters just mentioned. As pointed out in reference 25, a tremendous amount of data must be obtained and then manipulated even for a single valued nonlinearity such as saturation.

The procedure of deriving the families of the DIDF plots is as follows. First of all the value of 'n' is assumed and held fixed. Then for a fixed value of I, β is changed, while the computation of the DIDF is carried out for values of ϕ between zero and 2π. A digital computer is necessary to compute the DIDF and a representative flow chart is shown in Figure 28.

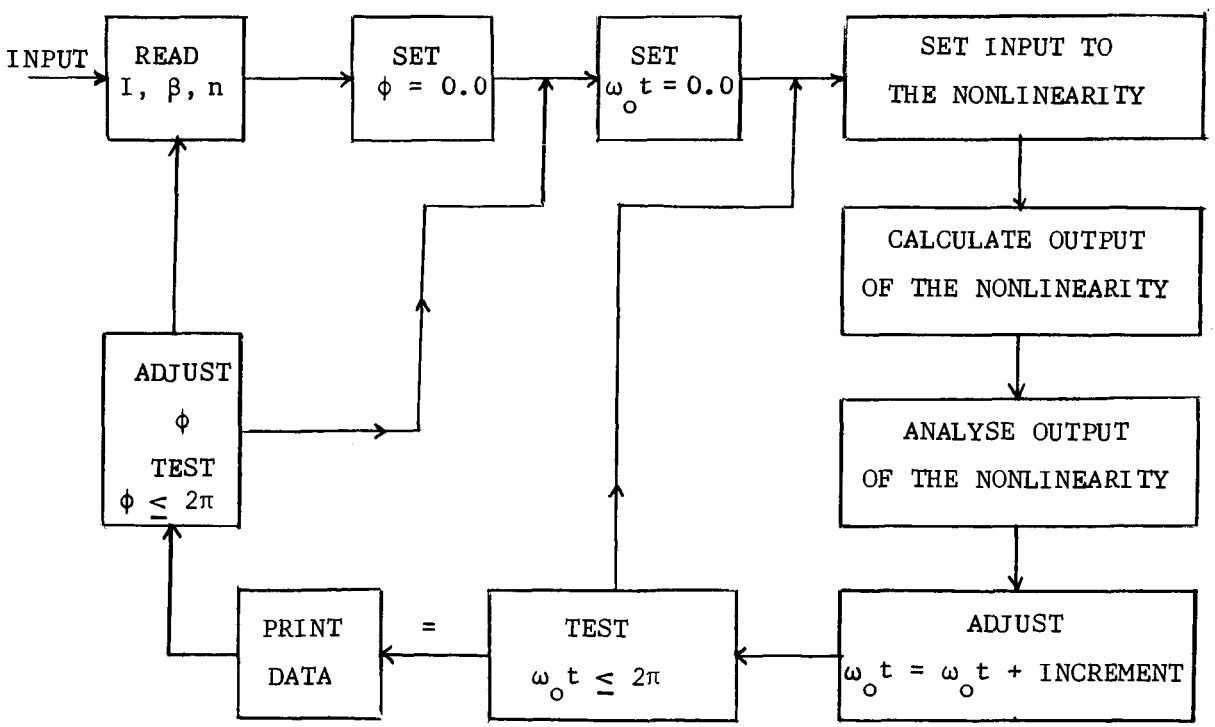

Figure 28 - A Flow Chart Indicating The Computation of DIDF

The use of the DIDF can be indicated by considering a control system shown in Figure 26.

(1) Stability of the forced oscillations: - Let the input to the system of Figure 26 be $r(t) = R \sin \omega_o t$ and then evaluate $c(t)$ and $e(t)$ by the conventional describing function method. Let $e(t) = I \sin (\omega_o t + \phi)$. To investigate the stability of the evaluated steady state solution, the feed back loop is broken, but a signal $c(t)$ equal to the steady state solution is injected back to the system. In addition to this signal, a small signal of frequency $n\omega_o/2\pi$ is also injected which gives rise to the output $c(t) + \delta \cos (n\omega_o t + \gamma)$. The evaluation of $\delta \cos (n\omega_o t + \gamma)$ is accomplished through the known DIDF of the nonlinearity. As n is varied both δ and γ vary, and may be plotted on the complex plane. If this gain locus encloses (-1,0) point, any slight disturbance will initiate oscillations of increasing amplitude, so that the steady state conditions assumed initially are unstable or divergent.

(2) Sub-Harmonic Oscillations: - The response of a nonlinear system to a sinusoidal signal, sometimes can be modified in amplitude and phase by the presence of the sinusoid of a harmonically related frequency. This effect modifies the loop gain of the system, and may make the closed loop continuously oscillatory; the frequency of oscillation being harmonically related to the input frequency. The DIDF enables the occurence of the subharmonic oscillations to be predicted quantitively. Since the frequency of the subharmonic oscillation is of the order of the

natural frequency of the linear system, the system response is small at the input frequency considered. The first step in predicting the subharmonic oscillations is to break the feed back loop and inject a subharmonic signal of frequency $\frac{1}{3}\omega_o$, $\frac{1}{5}\omega_o$, etc. For the system to oscillate continuously at a subharmonic frequency, the over all open loop gain for this low frequency component must be unity. For a fixed amplitude of the input signal, the DIDF family is known for various amplitudes of the signal at the subharmonic frequency. This information is available when the DIDF of the nonlinearity is evaluated. This DIDF family is then superimposed on the open loop frequency response of the linear system. The locus of the DIDF of a particular amplitude of the subharmonic signal which intersects the linear system locus at the subharmonic frequency determines the amplitude of the possible oscillations of the system at the subharmonic frequency.

The DIDF may be used to calculate the harmonic content of forced oscillations. There remains, however, the problem of computing and manipulating a mass of data while deriving the dual input describing function. Also the DIDF can be employed only when the sine waves are harmonically related.

Approximate DIDF, Boyer's Method: Boyer[24] has suggested an approximate dual input describing function which can be used to evaluate the stability of the forced oscillations. The derivation of the approximate DIDF has been confined to simple single valued nonlinearities having no energy storage elements. The derivation of the approximate DIDF is achieved in three steps. Let the input to the nonlinearity be $x(t) = I \sin \omega_o t + B \sin \beta t$,

where $\beta >> \omega_o$.

(1) The first step is to develop an equivalent gain of the nonlinearity under consideration. This is accomplished by applying a sine wave plus a d-c component to the nonlinearity. That is, let $\omega_o = 0$ and $I = A_o$ or $x = A_o + B \sin \beta t$. Then the output of the nonlinearity can be represented by,

$$\text{output} = A_v + B' \sin \beta t + B'' \cos \beta t + - - -$$

The equivalent gain is defined by,

$$K(A_o, B) = \frac{A_v}{A_o}$$

(2) Next the representative output of the nonlinearity is obtained by considering the input as $x = I \sin \omega_o t + B \sin \beta t$. Since $\beta >> \omega_o$, the value of the ω_o component in the input may be considered constant over a cycle of the β component. This constant value corresponds to a certain value of A_o, and the corresponding equivalent gain is known from step (1). So a plot of A_v versus $\omega_o t$ for the given nonlinearity can be constructed with B as a parameter. This is called the representative output. Note that the representative output is not the actual output of the nonlinearity.

(3) The last step is to obtain the fundamental component of the representative output by Fourier Analysis. Since the wave shape is known, but its equation may not be known, the approach for finding the fundamental component may be a graphical or trignometric. The ratio of this component to the amplitude of the ω_o component which is I, gives the magnitude of the approximate DIDF. For the single valued nonlinearities considered by

Boyer[24], the approximate DIDF are in general functions of I and B. For B = 0 the approximate DIDF reduces to the conventional describing function.

To illustrate the application of the approximate DIDF consider the control system shown in Figure 24. The input to the nonlinearity is $r = R \sin \omega_o t$ and the object is to determine the values of R and the corresponding values of ω_o for which the system is unstable. The first step is to plot the Nyquist plot of the linear system G_L, and then the Nyquist plot of $(- \frac{1}{DIDF})$ for values of B which will intersect the linear system Nyquist plot when superimposed. The value of B and the value of approximate DIDF at such an intersection, uniquely determines the value of I, since the approximate DIDF is a function of I and B only. Knowing I and the value of the approximate DIDF of the nonlinearity, the output c(t) is known. With a simple closed loop calculation this can be related to the input amplitude R and frequency ω_o. This, in turn, determines the value of the amplitude and frequency for which the system would be unstable. It is impossible to determine the stability of the forced oscillations or the occurence of the subharmonic oscillations by the conventional describing function. But the derivation of the exact dual-input describing function or even the approximate dual-input describing function for the nonlinearities containing an energy storage element, appears to be a most difficult if not an impossible task. A computer simulation provides a simpler mechanism than the DIDF for investigating the stability of forced oscillations and the presence of subharmonic oscillations.

CHAPTER VII

CONCLUSIONS

The describing function method constitutes an example of the application of a quasi-linear method for the evaluation of a nonlinear system performance. The method yields substantially accurate results for a certain class of nonlinear systems in which the linear portion of the system essentially acts as a low pass filter. The families of describing function curves shown in Figure 5 through Figure 11 and Figure 15 through Figure 20, make it relatively easy to predict the behavior of servomechanisms which contain either a deadzone and backlash separated by a first order linear block or a hysteresis relay and backlash separated by a second order linear block. These curves should be of definite aid to the control system engineer who is confronted with analyzing a system containing one of these particular nonlinearities. The generated describing function curves are not only a valuable tool for predicting the stability of a servomechanism containing such nonlinearities but also finding the proper network to improve the system performance. They are also useful in some cases where the performance of a linear system may be improved by purposely introducing a nonlinearity in one of the components.

Although only two sample problems are given, there are several ways in which the curves can be used in a problem analysis. For instance the internal gain of the linear block between the two nonlinearities exerts considerable influence over the effective backlash width. Thus in addition to controlling the overall system gain K, an additional factor must be considered in using K. Also, the time constant τ or zeta and ω_n in H(s) can be used as design parameters.

In the sample problems application, the generated describing function curves for analyzing control systems containing the multiple nonlinearities, have indicated that reasonably accurate predictions of the amplitude and frequency of the limit cycles can be made. This implies that the presence of the harmonic components at the input of the multiple nonlinearity does not modify the gain of the fundamental component appreciably. It cannot be over stressed that this is not a general result, because when the linear element in series with the multiple nonlinearity does not constitute a low pass filter, then the circulating harmonics may excessively distort the gain of the fundamental component. With this in mind, it would not be difficult to produce a system in which the method would not produce sensibly accurate results. Overall, the generated describing functions are so straight forward in application that having predicted the oscillation parameters, the accuracy of prediction may be assessed by estimating the harmonic distortion present under the predicted conditions.

The technique presented here for obtaining the describing functions of a particular nonlinear function can be used in obtaining the describing functions of any other nonlinear combinations. Therefore, it can be placed alongside of the other nonlinear anlytical tools in the servomechanism engineer's bag of tricks.

Table I - Magnitude and Phase Angle of the Describing Function of the First Multiple Nonlinearity for Various Values of Nondimensionalized Frequency $\tau\omega_o$, Normalized Ratio δ/I and $\frac{\delta K}{W} = 1$.

	$\delta/I = 0.05$		$\delta/I = 0.15$		$\delta/I = 0.25$		$\delta/I = 0.35$		$\delta/I = 0.45$		$\delta/I = 0.55$	
$\tau\omega_o$	ϕ, Degrees	G_D	ϕ, Degrees	G_D	ϕ, Degrees	G_D	ϕ, Degrees	G_D	ϕ, Degrees	G_D	ϕ, Degrees	G_D
0.0	-1.912	0.930	-6.496	0.781	-12.801	0.629	-22.393	0.482	-38.549	0.356	-57.399	0.218
0.1	-7.634	0.926	-12.234	0.777	-18.577	0.625	-28.217	0.480	-44.467	0.354	-63.342	0.212
0.2	-13.261	0.912	-17.929	0.765	-24.367	0.615	-34.170	0.471	-50.705	0.347	-69.122	0.194
0.4	-23.858	0.863	-28.792	0.722	-35.601	0.579	-46.052	0.442	-62.771	0.314	-79.848	0.144
0.6	-33.188	0.796	-38.538	0.665	-45.961	0.531	-57.243	0.402	-72.203	0.258	-90.800	0.091
0.8	-41.101	0.724	-46.978	0.602	-55.189	0.479	-66.838	0.351	-81.088	0.202	-103.071	0.041
1.0	-47.695	0.655	-54.186	0.542	-63.147	0.426	-74.723	0.296	-89.748	0.151		
2.0	-67.664	0.411	-77.414	0.322	-89.372	0.218	-105.601	0.101				
3.0	-77.445	0.286	-90.498	0.206	-106.925	0.109	-142.013	0.002				
4.0	-83.514	0.216	-100.056	0.139	-123.036	0.047						
5.0	-87.904	0.171	-108.230	0.097	-144.183	0.007						

Table II - Magnitude and Phase Angle of the Describing Function of the First Multiple Nonlinearity for Various Values of Nondimensionalized Frequency $\tau\omega_o$, Normalized Ratio δ/I and $\frac{\delta K}{W} = 2$.

	$\delta/I = 0.10$		$\delta/I = 0.20$		$\delta/I = 0.30$		$\delta/I = 0.40$		$\delta/I = 0.50$		$\delta/I = 0.60$	
$\tau\omega_o$	ϕ, Degrees	$\lvert G_D \rvert$	ϕ, Degrees	$\lvert G_D \rvert$	ϕ, Degrees	$\lvert G_D \rvert$	ϕ, Degrees	$\lvert G_D \rvert$	ϕ, Degrees	$\lvert G_D \rvert$	ϕ, Degrees	$\lvert G_D \rvert$
0.0	-2.052	0.867	-4.746	0.731	-8.518	0.596	-14.207	0.467	-23.591	0.348	-40.403	0.250
0.1	-7.779	0.863	-10.484	0.727	-14.275	0.593	-20.004	0.464	-29.438	0.346	-46.323	0.249
0.2	-13.406	0.850	-16.150	0.716	-19.997	0.584	-25.816	0.457	-35.406	0.340	-52.564	0.245
0.4	-24.010	0.804	-26.915	0.677	-30.989	0.552	-37.164	0.431	-47.335	0.322	-65.097	0.226
0.6	-33.354	0.742	-36.504	0.624	-40.940	0.508	-47.670	0.398	-58.585	0.296	-74.900	0.187
0.8	-41.285	0.675	-44.760	0.568	-49.669	0.462	-57.054	0.361	-68.491	0.261	-82.766	0.144
1.0	-47.900	0.611	-51.735	0.512	-57.171	0.416	-65.199	0.322	-76.259	0.220	-90.277	0.105
2.0	-67.996	0.383	-73.888	0.314	-81.312	0.240	-90.865	0.158	-104.378	0.071		
3.0	-77.892	0.267	-85.538	0.208	-95.062	0.143	-107.972	0.072				
4.0	-84.031	0.200	-93.554	0.148	-105.677	0.088	-124.752	0.024				
5.0	-88.503	0.158	-99.962	0.109	-115.201	0.053						

Table III - Magnitude and Phase Angle of the Describing Function of the First Multiple Nonlinearity for Various Values of Nondimensionalized Frequency $\tau\omega_o$, Normalized Ratio δ/I and $\frac{\delta K}{W} = 3$.

	$\delta/I = 0.15$		$\delta/I = 0.30$		$\delta/I = 0.45$		$\delta/I = 0.60$		$\delta/I = 0.75$	
$\tau\omega_o$	ϕ, Degrees	$\lvert G_D \rvert$	ϕ, Degrees	$\lvert G_D \rvert$	ϕ, Degrees	$\lvert G_D \rvert$	ϕ, Degrees	$\lvert G_D \rvert$	ϕ, Degrees	$\lvert G_D \rvert$
0.0	-2.213	0.804	-5.707	0.608	-12.073	0.422	-26.214	0.259	-62.605	0.157
0.1	-7.935	0.800	-11.451	0.605	-17.839	0.420	-32.058	0.258	-68.055	0.150
0.2	-13.568	0.788	-17.131	0.596	-23.623	0.413	-38.074	0.254	-72.953	0.134
0.4	-24.182	0.746	-27.957	0.563	-34.854	0.391	-50.087	0.242	-81.568	0.095
0.6	-33.544	0.688	-37.641	0.520	-45.147	0.361	-61.426	0.223	-89.698	0.061
0.8	-41.494	0.626	-46.020	0.473	-54.301	0.330	-71.471	0.197	-98.601	0.031
1.0	-48.133	0.567	-53.151	0.428	-62.243	0.297	-79.010	0.163	-110.198	0.006
2.0	-68.376	0.356	-75.960	0.261	-87.162	0.157	-106.082	0.044		
3.0	-78.410	0.247	-87.909	0.168	-102.070	0.081				
4.0	-84.629	0.185	-96.287	0.115	-114.851	0.038				
5.0	-89.152	0.145	-103.217	0.082	-129.569	0.011				

Table IV - Magnitude and Phase Angle of the Describing Function of the First Multiple Nonlinearity for Various Values of Nondimensionalized Frequency $\tau\omega_o$, Normalized Ratio δ/I and $\frac{\delta K}{W} = 4$.

	$\delta/I = 0.20$		$\delta/I = 0.40$		$\delta/I = 0.60$	
$\tau\omega_o$	ϕ, Degrees	$\lvert G_D \rvert$	ϕ, Degrees	$\lvert G_D \rvert$	ϕ, Degrees	$\lvert G_D \rvert$
0.0	-2.400	0.741	-7.094	0.490	-19.409	0.266
0.1	-8.132	0.738	-12.845	0.487	-25.206	0.264
0.2	-13.763	0.727	-18.547	0.480	-31.112	0.260
0.4	-24.386	0.687	-29.465	0.454	-42.765	0.248
0.6	-33.766	0.635	-39.280	0.419	-53.641	0.231
0.8	-41.740	0.578	-47.829	0.382	-63.398	0.210
1.0	-48.404	0.523	-55.154	0.346	-71.916	0.186
2.0	-68.813	0.328	-78.731	0.208	-96.536	0.075
3.0	-78.977	0.228	-90.986	0.128	-115.516	0.020
4.0	-85.272	0.170	-99.855	0.083		
5.0	-89.904	0.132	-107.467	0.055		

Table V - Magnitude and Phase Angle of the Describing Function of the First Multiple Nonlinearity for Various Values of Nondimensionalized Frequency $\tau\omega_o$, Normalized Ratio δ/I and $\frac{\delta K}{W} = \frac{1}{2}$.

	$\delta/I = 0.05$		$\delta/I = 0.10$		$\delta/I = 0.20$		$\delta/I = 0.30$		$\delta/I = 0.35$		$\delta/I = 0.40$	
$\tau\omega_o$	ϕ, Degrees	$\lvert G_D \rvert$	ϕ, Degrees	$\lvert G_D \rvert$	ϕ, Degrees	G_D	ϕ, Degrees	G_D	ϕ, Degrees	G_D	ϕ, Degrees	G_D
0.0	-3.770	0.920	-7.947	0.829	-18.618	0.638	-35.740	0.458	-46.657	0.368	-55.045	0.249
0.1	-9.497	0.915	-13.704	0.825	-24.434	0.634	-41.689	0.455	-52.421	0.361	-61.103	0.242
0.2	-15.152	0.901	-19.416	0.812	-30.310	0.623	-47.813	0.444	-57.932	0.343	-67.258	0.225
0.4	-25.856	0.852	-30.355	0.765	-41.904	0.583	-59.296	0.397	-68.543	0.286	-79.135	0.168
0.6	-35.348	0.785	-40.211	0.703	-52.798	0.529	-69.491	0.333	-79.291	0.222	-91.877	0.105
0.8	-43.462	0.713	-48.803	0.635	-62.307	0.466	-79.348	0.266	-90.346	0.156	-106.388	0.041
1.0	-50.290	0.643	-56.193	0.569	-70.458	0.401	-88.833	0.202	-101.605	0.094		
2.0	-71.665	0.396	-80.402	0.329	-101.121	0.165						
3.0	-82.935	0.269	-94.814	0.203	-127.767	0.043						
4.0	-90.526	0.196	-105.952	0.130								
5.0	-96.462	0.150	-115.895	0.083								

Table VI - Magnitude and Phase Angle of the Describing Function of the First Multiple Nonlinearity for Various Values of Nondimensionalized Frequency $\tau\omega_o$, Normalized Ratio δ/I and $\frac{\delta K}{W} = \frac{1}{3}$.

	$\delta/I = 0.05$		$\delta/I = 0.10$		$\delta/I = 0.15$		$\delta/I = 0.20$		$\delta/I = 0.25$		$\delta/I = 0.30$	
$\tau\omega_o$	ϕ, Degrees	$\lvert G_D \rvert$	ϕ, Degrees	$\lvert G_D \rvert$	ϕ, Degrees	$\lvert G_D \rvert$	ϕ, Degrees	$\lvert G_D \rvert$	ϕ, Degrees	$\lvert G_D \rvert$	ϕ, Degrees	$\lvert G_D \rvert$
0.0	-5.591	0.907	-11.773	0.796	-19.094	0.679	-28.387	0.562	-41.061	0.454	-50.681	0.309
0.1	-11.326	0.902	-17.537	0.791	-24.887	0.674	-34.281	0.559	-46.668	0.447	-56.746	0.303
0.2	-17.006	0.888	-23.304	0.778	-30.772	0.662	-40.330	0.547	-52.070	0.429	-62.800	0.285
0.4	-27.810	0.839	-34.452	0.731	-42.382	0.618	-52.308	0.503	-62.903	0.371	-74.679	0.226
0.6	-37.462	0.772	-44.668	0.668	-53.280	0.559	-63.003	0.437	-73.930	0.302	-87.116	0.158
0.8	-45.770	0.699	-53.716	0.599	-62.752	0.489	-72.876	0.365	-84.6[illegible]	0.230	-100.691	0.086
1.0	-52.837	0.629	-61.511	0.531	-71.089	0.419	-82.041	0.295	-95.429	0.161	-118.322	0.018
2.0	-75.529	0.378	-88.248	0.281	-103.131	0.169	-124.628	0.045				
3.0	-88.239	0.248	-106.224	0.150	-132.033	0.037						
4.0	-97.344	0.173	-122.084	0.074								
5.0	-104.921	0.126	-139.872	0.024								

Table VII - Magnitude and Phase Angle of the Describing Function of the First Multiple Nonlinearity for Various Values of Nondimensionalized Frequency $\tau\omega_o$, Normalized Ratio δ/I and $\frac{\delta K}{W} = \frac{1}{4}$.

	δ/I = 0.05		δ/I = 0.10		δ/I = 0.15		δ/I = 0.20		δ/I = 0.25		δ/I = 0.30	
$\tau\omega_o$	ϕ, Degrees	$\lvert G_D \rvert$	ϕ, Degrees	$\lvert G_D \rvert$	ϕ, Degrees	$\lvert G_D \rvert$	ϕ, Degrees	G_D	ϕ, Degrees	G_D	ϕ, Degrees	G_D
0.0	-7.383	0.892	-15.581	0.758	-25.624	0.618	-39.283	0.483	-50.681	0.309	-65.565	0.126
0.1	-13.132	0.887	-21.376	0.754	-31.490	0.614	-44.891	0.476	-56.765	0.303	-71.963	0.120
0.2	-18.839	0.873	-27.200	0.741	-37.485	0.602	-50.412	0.457	-62.941	0.285	-79.025	0.102
0.4	-29.741	0.823	-38.573	0.693	-49.417	0.555	-61.519	0.399	-75.231	0.225	-95.902	0.041
0.6	-39.538	0.756	-49.138	0.629	-60.277	0.488	-72.756	0.327	-88.489	0.154		
0.8	-48.043	0.682	-58.492	0.558	-70.182	0.413	-83.848	0.252	-102.965	0.078		
1.0	-55.342	0.612	-66.629	0.487	-79.256	0.341	-94.648	0.179	-124.592	0.006		
2.0	-79.270	0.357	-96.306	0.228	-118.857	0.079						
3.0	-93.485	0.224	-118.910	0.092	-132.033	0.037						
4.0	-104.237	0.148	-146.523	0.012								
5.0	-113.764	0.099										

Table VIII - Magnitude and Phase Angle of the Describing Function of the Second Multiple Nonlinearity for the Nondimensionalized Frequency ω_o/ω_n, Zeta and K/W = 1.

Zeta		ω_o/ω_n =.075	ω_o/ω_n =.1	ω_o/ω_n =.2	ω_o/ω_n =.3	ω_o/ω_n =.4	ω_o/ω_n =.5	ω_o/ω_n =.6	ω_o/ω_n =.7	ω_o/ω_n =.8	ω_o/ω_n =.9	ω_o/ω_n =1.0	ω_o/ω_n =1.1	ω_o/ω_n =1.2
.05	$\lvert G_D \rvert$	1.276	1.288	1.331	1.373	1.464	1.530	1.755	2.233	3.224	5.863	12.573	5.158	2.507
	ϕ	-.548	-4.191	-1.892	-5.517	-16.521	-25.385	-23.259	-21.874	-22.566	-31.120	-92.781	-158.807	-176.748
.1	$\lvert G_D \rvert$	1.219	1.262	1.335	1.372	1.495	1.544	1.745	2.173	2.999	4.647	6.146	3.959	2.255
	ϕ	-.177	-2.482	-5.192	-5.935	-21.910	-29.296	-28.798	-29.807	-34.652	-50.554	-95.425	-141.909	-164.622
.15	$\lvert G_D \rvert$	1.239	1.243	1.301	1.387	1.524	1.543	1.709	2.071	2.694	3.594	3.987	3.005	1.947
	ϕ	-2.543	-4.252	-8.589	-7.332	-27.039	-33.175	-34.219	-37.395	-45.305	-63.595	-98.010	-132.989	-155.701
.2	$\lvert G_D \rvert$	1.318	1.241	1.312	1.434	1.541	1.521	1.650	1.933	2.363	2.822	2.900	2.340	1.653
	ϕ	-3.504	-3.484	-7.795	-11.491	-31.406	-36.958	-39.402	-44.377	-54.270	-72.654	-100.562	-128.525	-149.686
.3	$\lvert G_D \rvert$	1.455	1.570	1.554	1.547	1.475	1.389	1.457	1.600	1.763	1.862	1.801	1.531	1.183
	ϕ	-6.560	-9.097	-18.392	-26.539	-38.277	-43.205	-48.248	-55.976	-67.874	-84.911	-105.651	-126.006	-143.644
.4	$\lvert G_D \rvert$	1.135	1.252	1.257	1.271	1.219	1.191	1.224	1.280	1.320	1.324	1.246	1.070	.858
	ϕ	-7.040	-9.865	-10.762	-29.824	-40.107	-47.633	-55.460	-65.327	-78.120	-93.813	-110.908	-127.365	-142.579
.5	$\lvert G_D \rvert$	.997	.998	1.044	1.033	1.012	1.001	1.009	1.020	1.018	.991	.909	.779	.627
	ϕ	-7.881	-10.897	-21.486	-32.171	-42.724	-52.158	-62.019	-73.457	-86.733	-101.506	-116.341	-130.718	-144.268
.8	$\lvert G_D \rvert$	.673	.673	.668	.659	.646	.631	.612	.584	.537	.475	.398	.315	.227
	ϕ	-10.799	-13.720	-27.761	-41.580	-55.273	-69.152	-83.006	-96.796	-109.943	-122.647	-134.934	-146.944	-158.738

ϕ is in Degrees

Table IX - Magnitude and Phase Angle of the Describing Function of the Second Multiple Nonlinearity for the Nondimensionalized Frequency ω_o/ω_n, Zeta and K/W = 3.

Zeta		ω_o/ω_n =.075	ω_o/ω_n =.1	ω_o/ω_n =.2	ω_o/ω_n =.3	ω_o/ω_n =.4	ω_o/ω_n =.5	ω_o/ω_n =.6	ω_o/ω_n =.7	ω_o/ω_n =.8	ω_o/ω_n =.9	ω_o/ω_n =1.0	ω_o/ω_n =1.1	ω_o/ω_n =1.2
.05	$\lvert G_D \rvert$	1.287	1.285	1.327	1.391	1.511	1.662	1.936	2.425	3.407	6.019	12.697	5.328	2.732
	ϕ	-.597	-1.828	-1.377	-3.179	-6.074	-10.945	-11.391	-12.617	-15.974	-27.323	-90.942	-154.572	-168.940
.1	$\lvert G_D \rvert$	1.285	1.288	1.329	1.389	1.514	1.662	1.918	2.364	3.188	4.822	6.316	4.141	2.483
	ϕ	-1.119	-2.217	-2.966	-4.803	-9.098	-14.792	-16.758	-20.304	-27.647	-45.901	-91.859	-136.509	-156.014
.15	$\lvert G_D \rvert$	1.275	1.285	1.327	1.385	1.516	1.654	1.883	2.268	2.898	3.804	4.186	3.204	2.180
	ϕ	-1.097	-2.924	-4.714	-6.335	-12.271	-18.585	-21.991	-27.556	-37.729	-57.924	-92.764	-126.103	-145.943
.2	$\lvert G_D \rvert$	1.306	1.308	1.332	1.385	1.514	1.637	1.835	2.148	2.593	3.061	3.117	2.555	1.893
	ϕ	-2.154	-3.374	-7.418	-7.854	-15.563	-22.304	-27.024	-34.228	-46.102	-65.874	-93.650	-120.021	-138.493
.3	$\lvert G_D \rvert$	1.205	1.206	1.286	1.392	1.504	1.578	1.705	1.875	2.048	2.134	2.046	1.772	1.442
	ϕ	-2.053	-2.450	-7.089	-12.140	-22.917	-29.438	-36.275	-45.587	-58.505	-75.615	-95.404	-113.984	-129.150
.4	$\lvert G_D \rvert$	1.328	1.349	1.371	1.426	1.464	1.490	1.543	1.599	1.630	1.608	1.508	1.332	1.132
	ϕ	-4.519	-5.871	-12.237	-19.643	-28.783	-36.061	-44.246	-54.314	-66.818	-81.602	-97.149	-111.622	-124.232
.5	$\lvert G_D \rvert$	1.419	1.415	1.415	1.408	1.387	1.365	1.358	1.353	1.333	1.281	1.185	1.056	.917
	ϕ	-6.410	-8.500	-16.634	-25.363	-33.957	-41.805	-50.482	-60.870	-72.938	-85.980	-98.908	-110.920	-121.717
.8	$\lvert G_D \rvert$	1.095	1.095	1.082	1.061	1.032	.996	.955	.904	.842	.774	.700	.626	.555
	ϕ	-7.983	-10.789	-21.701	-32.522	-43.141	-53.881	-64.722	-75.340	-85.525	-95.225	-104.287	-112.786	-120.723

ϕ is in Degrees

Table X - Magnitude and Phase Angle of the Describing Function of the Second Multiple Nonlinearity for the Nondimensionalized Frequency ω_o/ω_n, Zeta and K/W = 5.

Zeta		ω_o/ω_n =.075	ω_o/ω_n =.1	ω_o/ω_n =.2	ω_o/ω_n =.3	ω_o/ω_n =.4	ω_o/ω_n =.5	ω_o/ω_n =.6	ω_o/ω_n =.7	ω_o/ω_n =.8	ω_o/ω_n =.9	ω_o/ω_n =1.0	ω_o/ω_n =1.1	ω_o/ω_n =1.2
.05	$\lvert G_D \rvert$	1.281	1.285	1.326	1.394	1.513	1.680	1.960	2.451	3.432	6.039	12.716	5.351	2.764
	ϕ	-.839	-1.434	-1.193	-2.737	-4.699	-8.100	-8.998	-10.721	-14.614	-26.539	-90.569	-153.696	-160.298
.1	$\lvert G_D \rvert$	1.281	1.284	1.327	1.391	1.515	1.676	1.940	2.388	3.212	4.846	6.341	4.166	2.513
	ϕ	-1.297	-1.633	-2.563	-4.500	-7.528	-11.918	-14.321	-18.346	-26.192	-44.934	-91.124	-135.389	-154.198
.15	$\lvert G_D \rvert$	1.281	1.286	1.328	1.387	1.511	1.664	1.904	2.291	2.923	3.832	4.214	3.231	2.212
	ϕ	-1.296	-1.933	-4.113	-6.168	-10.540	-15.677	-19.499	-25.509	-36.137	-56.723	-91.672	-124.672	-143.895
.2	$\lvert G_D \rvert$	1.249	1.267	1.326	1.384	1.506	1.645	1.854	2.172	2.622	3.097	3.149	2.585	1.927
	ϕ	-.674	-2.117	-5.812	-7.713	-13.356	-19.353	-24.454	-32.069	-44.350	-64.436	-92.216	-118.248	-136.157
.3	$\lvert G_D \rvert$	1.279	1.271	1.307	1.378	1.488	1.586	1.726	1.907	2.088	2.193	2.083	1.806	1.477
	ϕ	-3.095	-3.766	-8.015	-11.469	-19.724	-26.380	-33.537	-43.201	-56.443	-73.678	-93.286	-111.506	-126.128
.4	$\lvert G_D \rvert$	1.247	1.270	1.310	1.387	1.453	1.506	1.577	1.647	1.681	1.655	1.549	1.370	1.171
	ϕ	-3.412	-4.490	-9.740	-16.582	-25.484	-32.877	-41.393	-51.840	-64.471	-79.112	-94.360	-108.420	-120.484
.5	$\lvert G_D \rvert$	1.339	1.339	1.359	1.383	1.397	1.415	1.416	1.411	1.386	1.347	1.227	1.097	.958
	ϕ	-5.211	-6.920	-14.004	-22.052	-30.513	-38.770	-47.920	-58.295	-70.154	-82.899	-95.408	-106.965	-117.192
.8	$\lvert G_D \rvert$	1.180	1.179	1.165	1.139	1.106	1.065	1.018	.960	.893	.821	.746	.672	.601
	ϕ	-7.625	-10.229	-20.665	-30.818	-40.963	-51.113	-61.392	-71.438	-81.063	-90.165	-98.632	-106.472	-113.708

ϕ is in Degrees

Table XI - Magnitude and Phase Angle of the Describing Function of the Second Multiple Nonlinearity for the Nondimensionalized Frequency ω_o/ω_n, Zeta and K/W = 7.

Zeta		ω_o/ω_n =.075	ω_o/ω_n =.1	ω_o/ω_n =.2	ω_o/ω_n =.3	ω_o/ω_n =.4	ω_o/ω_n =.5	ω_o/ω_n =.6	ω_o/ω_n =.7	ω_o/ω_n =.8	ω_o/ω_n =.9	ω_o/ω_n =1.0	ω_o/ω_n =1.1	ω_o/ω_n =1.2
.05	$\lvert G_D \rvert$	1.278	1.286	1.326	1.396	1.515	1.686	1.968	2.460	3.440	6.047	12.721	5.359	2.775
	ϕ	-.848	-1.221	-1.193	-2.481	-4.141	-6.878	-7.962	-9.901	-14.022	-26.202	-90.407	-153.315	-166.577
.10	$\lvert G_D \rvert$	1.287	1.285	1.325	1.393	1.513	1.700	1.947	2.397	3.220	4.853	6.350	4.174	2.524
	ϕ	-.766	-1.615	-2.526	-4.294	-6.879	-10.686	-13.273	-17.500	-25.561	-44.514	-90.806	-134.900	-153.408
.15	$\lvert G_D \rvert$	1.278	1.284	1.327	1.390	1.509	1.667	1.909	2.300	2.932	3.842	4.225	3.241	2.223
	ϕ	-1.344	-1.904	-3.822	-6.081	-9.740	-14.431	-18.419	-24.626	-35.448	-56.199	-91.202	-124.054	-142.998
.2	$\lvert G_D \rvert$	1.272	1.284	1.325	1.384	1.502	1.646	1.860	2.180	2.631	3.109	3.161	2.595	1.938
	ϕ	-1.518	-2.811	-5.312	-7.713	-12.550	-18.087	-23.346	-31.137	-43.583	-63.803	-91.592	-117.479	-135.128
.3	$\lvert G_D \rvert$	1.313	1.300	1.318	1.375	1.479	1.587	1.732	1.917	2.102	2.193	2.097	1.818	1.490
	ϕ	-3.396	-4.327	-8.499	-11.365	-18.364	-25.066	-32.350	-42.151	-55.524	-72.821	-92.369	-110.419	-124.814
.4	$\lvert G_D \rvert$	1.227	1.243	1.292	1.370	1.445	1.508	1.586	1.662	1.701	1.673	1.564	1.384	1.184
	ϕ	-3.120	-3.973	-9.114	-15.495	-24.083	-31.498	-40.120	-50.699	-63.439	-78.028	-93.131	-107.012	-118.839
.5	$\lvert G_D \rvert$	1.304	1.305	1.333	1.367	1.394	1.415	1.434	1.434	1.407	1.347	1.244	1.112	.973
	ϕ	-4.776	-6.306	-12.937	-20.684	-29.028	-37.337	-46.645	-57.155	-68.938	-81.543	-93.897	-105.235	-115.220
.8	$\lvert G_D \rvert$	1.216	1.215	1.199	1.173	1.137	1.094	1.044	.984	.914	.840	.763	.689	.618
	ϕ	-7.487	-10.014	-20.138	-30.157	-39.992	-49.957	-59.945	-69.795	-79.159	-88.002	-96.204	-103.756	-110.674

ϕ is in Degrees

Table XII - Magnitude and Phase Angle of the Describing Function of the Second Multiple Nonlinearity for the Nondimensionalized Frequency ω_o/ω_n, Zeta and K/W = 9.

Zeta		ω_o/ω_n =.075	ω_o/ω_n =.1	ω_o/ω_n =.2	ω_o/ω_n =.3	ω_o/ω_n =.4	ω_o/ω_n =.5	ω_o/ω_n =.6	ω_o/ω_n =.7	ω_o/ω_n =.8	ω_o/ω_n =.9	ω_o/ω_n =1.0	ω_o/ω_n =1.1	ω_o/ω_n =1.2
.05	$\lvert G_D \rvert$	1.277	1.286	1.326	1.397	1.515	1.689	1.973	2.464	3.444	6.050	12.724	5.363	2.780
	ϕ	-.761	-1.079	-1.193	-2.339	-3.772	-6.199	-7.390	-9.440	-13.695	-25.891	-90.317	-153.103	-166.177
.10	$\lvert G_D \rvert$	1.284	1.285	1.326	1.394	1.512	1.682	1.950	2.401	3.225	4.858	6.355	4.178	2.530
	ϕ	-.821	-1.531	-2.485	-4.155	-6.587	-9.999	-12.684	-17.024	-25.210	-44.281	-90.629	-134.628	-152.966
.15	$\lvert G_D \rvert$	1.286	1.286	1.325	1.389	1.508	1.667	1.912	2.303	2.936	3.847	4.230	3.245	2.229
	ϕ	-1.726	-2.210	-3.712	-5.996	-9.363	-13.736	-17.820	-24.128	-35.059	-55.906	-90.936	-123.704	-142.499
.2	$\lvert G_D \rvert$	1.285	1.293	1.325	1.385	1.499	1.646	1.862	2.183	2.636	3.118	3.168	2.600	1.944
	ϕ	-1.974	-3.033	-5.095	-7.701	-12.112	-17.384	-22.727	-30.612	-43.156	-63.448	-91.245	-117.047	-134.557
.3	$\lvert G_D \rvert$	1.307	1.302	1.320	1.374	1.474	1.585	1.735	1.921	2.109	2.202	2.104	1.825	1.496
	ϕ	-3.173	-4.239	-8.216	-11.262	-17.686	-24.337	-31.687	-41.563	-55.006	-72.349	-91.847	-109.817	-124.070
.4	$\lvert G_D \rvert$	1.245	1.258	1.295	1.364	1.440	1.508	1.590	1.669	1.711	1.682	1.572	1.391	1.191
	ϕ	-3.378	-4.287	-9.313	-15.224	-23.306	-30.730	-39.404	-50.043	-62.850	-77.414	-92.454	-106.230	-117.917
.5	$\lvert G_D \rvert$	1.284	1.286	1.317	1.357	1.391	1.418	1.441	1.446	1.419	1.357	1.252	1.119	.984
	ϕ	-4.524	-5.987	-12.357	-19.943	-28.208	-36.526	-45.898	-56.500	-68.265	-80.799	-93.046	-104.270	-114.107
.8	$\lvert G_D \rvert$	1.236	1.235	1.219	1.192	1.154	1.110	1.058	.996	.925	.850	.772	.697	.627
	ϕ	-7.413	-9.899	-19.858	-29.746	-39.475	-49.273	-59.171	-68.845	-78.095	-86.809	-94.859	-102.247	-108.989

ϕ is in Degrees

Table XIII - Magnitude and Phase Angle of the Describing Function of the Second Multiple Nonlinearity for the Nondimensionalized Frequency ω_o/ω_n, Zeta and K/W = 11.

Zeta		ω_o/ω_n =.075	ω_o/ω_n =.1	ω_o/ω_n =.2	ω_o/ω_n =.3	ω_o/ω_n =.4	ω_o/ω_n =.5	ω_o/ω_n =.6	ω_o/ω_n =.7	ω_o/ω_n =.8	ω_o/ω_n =.9	ω_o/ω_n =1.0	ω_o/ω_n =1.1	ω_o/ω_n =1.2
.05	$\lvert G_D \rvert$	1.277	1.286	1.326	1.397	1.515	1.691	1.975	2.467	3.447	6.051	12.726	5.365	2.783
	ϕ	-.692	-.988	-1.193	-2.248	-3.584	-5.768	-7.021	-9.147	-13.484	-25.891	-90.260	-152.969	-165.919
.1	$\lvert G_D \rvert$	1.283	1.286	1.326	1.395	1.512	1.683	1.952	2.403	3.226	4.860	6.358	4.181	2.532
	ϕ	-.777	-1.487	-2.453	-4.073	-6.378	-9.562	-12.311	-16.722	-24.983	-44.131	-90.516	-134.456	-152.681
.15	$\lvert G_D \rvert$	1.282	1.286	1.324	1.389	1.507	1.668	1.914	2.305	2.938	3.850	4.232	3.248	2.232
	ϕ	-1.434	-2.043	-3.685	-5.942	-9.133	-13.294	-17.437	-23.812	-34.811	-55.719	-90.767	-123.481	-142.177
.2	$\lvert G_D \rvert$	1.284	1.290	1.325	1.386	1.497	1.646	1.863	2.185	2.638	3.118	3.171	2.603	1.947
	ϕ	-1.910	-2.697	-4.981	-7.667	-11.886	-16.937	-22.332	-30.278	-42.881	-63.222	-91.020	-116.770	-134.187
.3	$\lvert G_D \rvert$	1.297	1.294	1.320	1.373	1.472	1.585	1.736	1.923	2.112	2.207	2.108	1.828	1.500
	ϕ	-2.918	-3.932	-7.983	-11.227	-17.303	-23.872	-31.263	-41.185	-54.669	-72.041	-91.518	-109.425	-123.600
.4	$\lvert G_D \rvert$	1.256	1.267	1.298	1.360	1.436	1.507	1.592	1.673	1.717	1.689	1.576	1.395	1.195
	ϕ	-3.538	-4.480	-9.466	-15.077	-22.816	-30.242	-38.944	-49.624	-62.466	-77.027	-92.010	-105.724	-117.327
.5	$\lvert G_D \rvert$	1.272	1.275	1.307	1.351	1.388	1.418	1.445	1.452	1.425	1.362	1.257	1.123	.984
	ϕ	-4.360	-5.780	-12.005	-19.467	-27.691	-36.007	-45.410	-56.062	-67.821	-80.309	-92.508	-103.649	-113.400
.8	$\lvert G_D \rvert$	1.249	1.248	1.231	1.203	1.166	1.120	1.066	1.003	.932	.855	0.777	0.702	.631
	ϕ	-7.368	-9.828	-19.684	-29.470	-39.155	-48.847	-58.661	-68.252	-77.427	-86.026	-93.981	-101.265	-107.892

ϕ is in Degrees

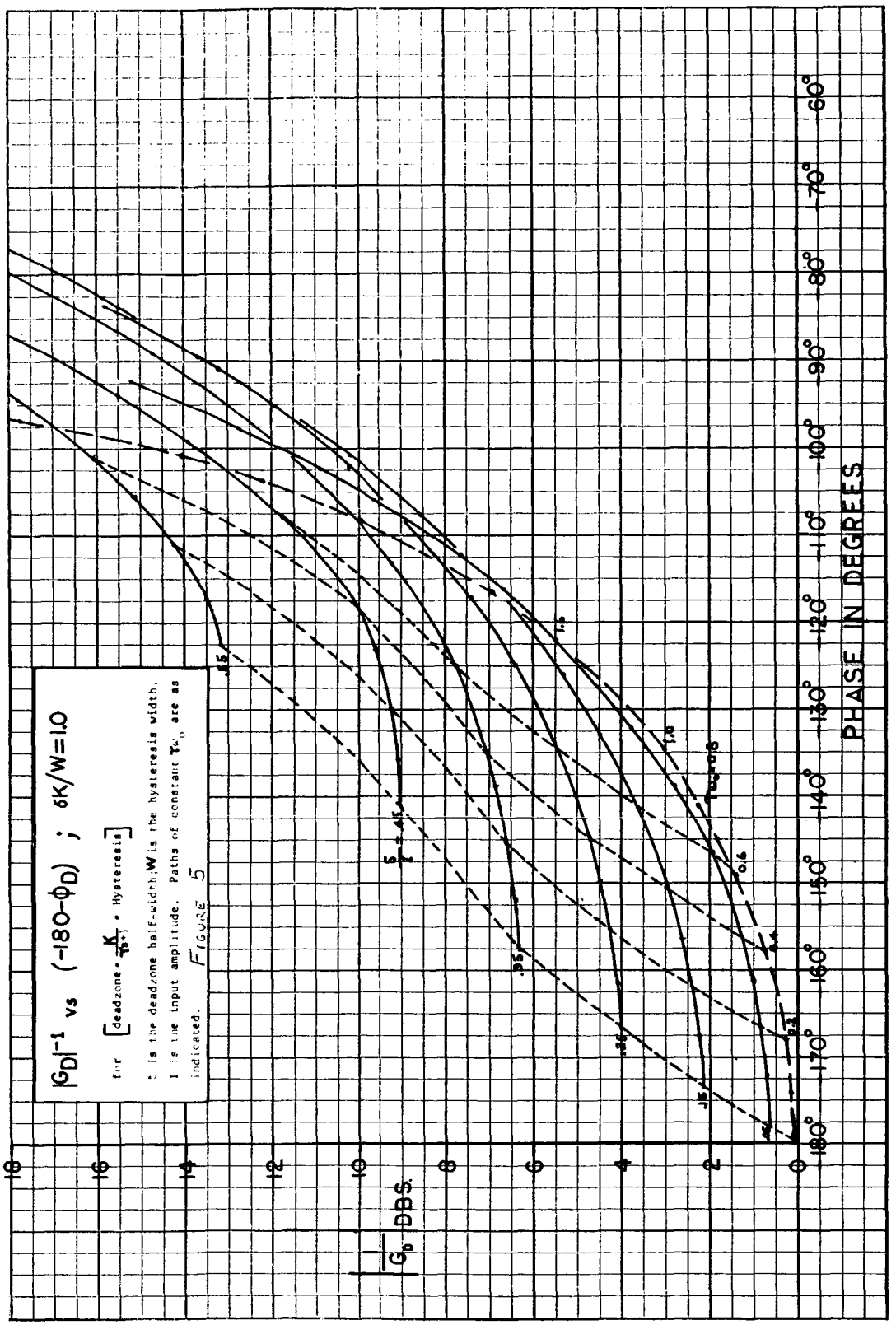
$|G_D|^{-1}$ vs $(-180-\phi_D)$; 6K/W=1.0
for [deadzone = $\frac{K}{\text{Hysteresis}}$]
δ is the deadzone half-width; W is the hysteresis width.
I is the input amplitude. Paths of constant τ_{ω_0} are as indicated.
FIGURE 5
$\frac{1}{|G_b|}$ DBS.
PHASE IN DEGREES
0
2
4
6
8
10
12
14
16
18
-180°
-170°
-160°
-150°
-140°
-130°
-120°
-110°
-100°
-90°
-80°
-70°
-60°
.15
.35
.25
.45
.8
1.0
1.5
.6
.4
.2

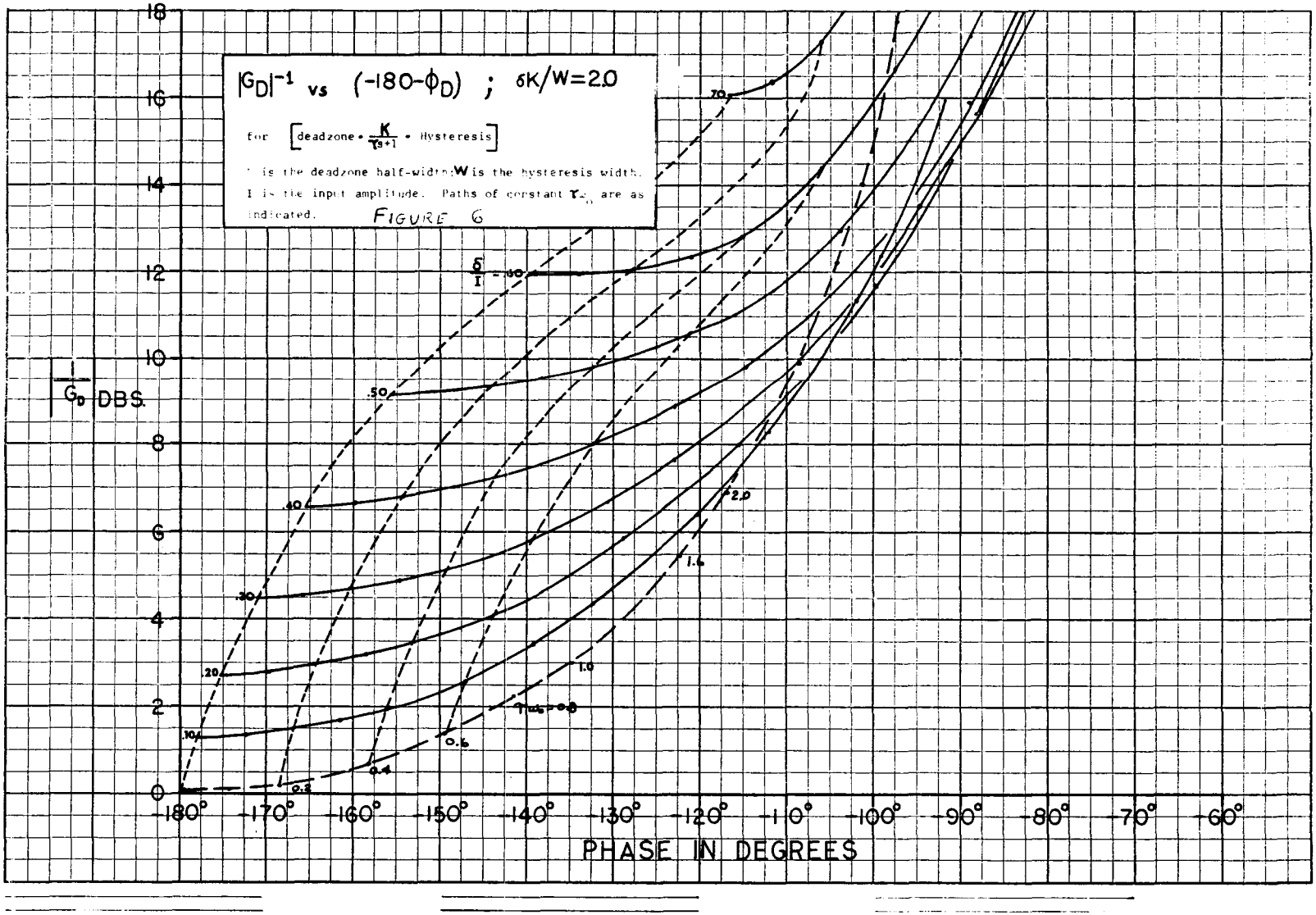
$|G_D|^{-1}$ vs $(-180-\phi_D)$; $\delta K/W=2.0$
for $\left[\text{deadzone} * \frac{K}{\tau s+1} * \text{Hysteresis}\right]$
δ is the deadzone half-width; W is the hysteresis width.
I is the input amplitude. Paths of constant τ_{ω_0} are as indicated.
FIGURE 6
$\frac{\delta}{I}$ = 1.00
.70
.50
.40
.30
.20
.10
2.0
1.6
1.0
τ_{ω_0}=0.8
0.6
0.4
0.2
$\frac{1}{G_D}$ DBS.
18
16
14
12
10
8
6
4
2
0
-180°
-170°
-160°
-150°
-140°
-130°
-120°
-110°
-100°
-90°
-80°
-70°
-60°
PHASE IN DEGREES

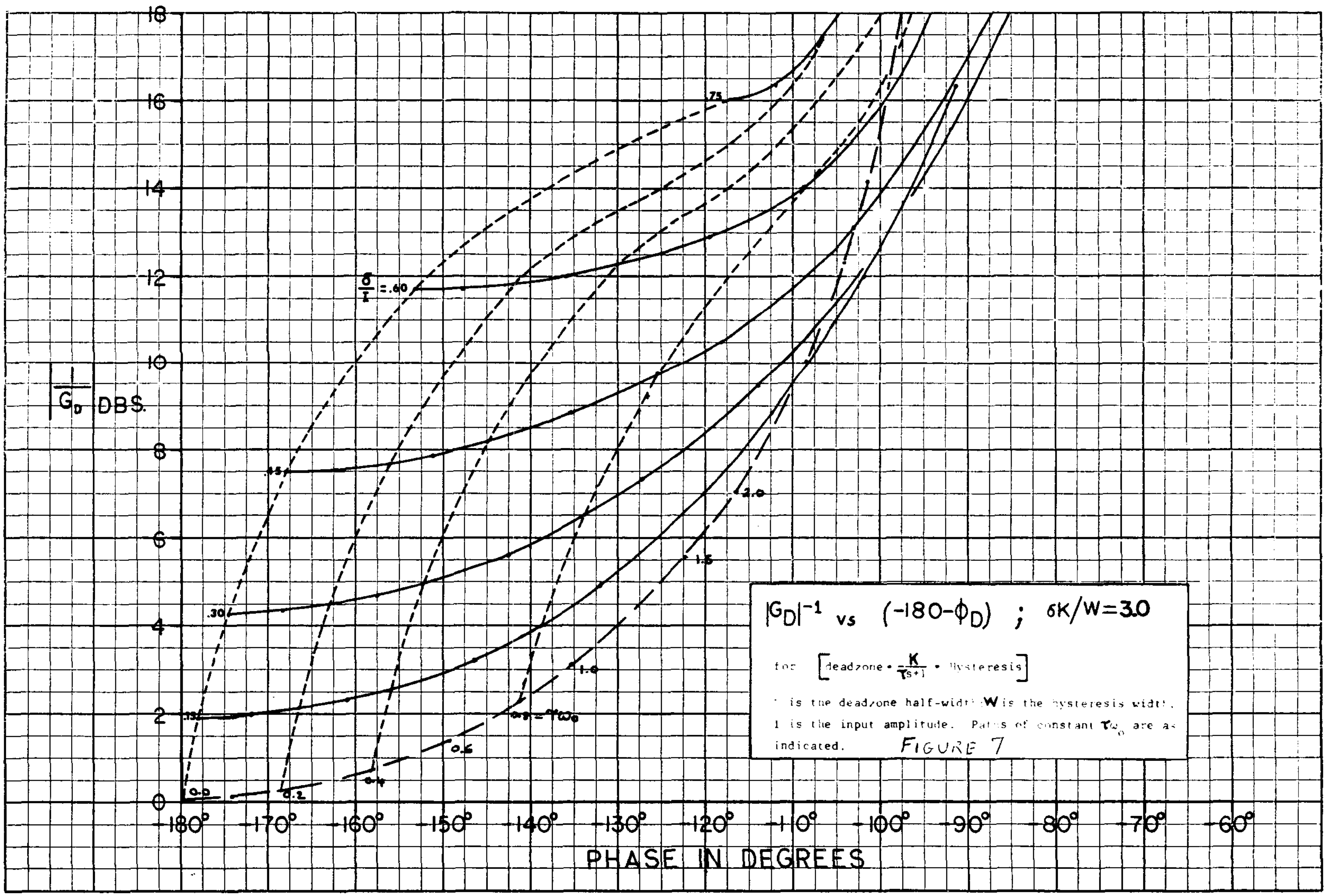

$|G_D|^{-1}$ vs $(-180-\phi_D)$; $\delta K/W = 3.0$

for $\left[\text{deadzone} \cdot \frac{K}{\tau s+1} \cdot \text{Hysteresis}\right]$

is the deadzone half-width. **W** is the hysteresis width. I is the input amplitude. Paths of constant $\tau\omega_0$ are as indicated.

FIGURE 7

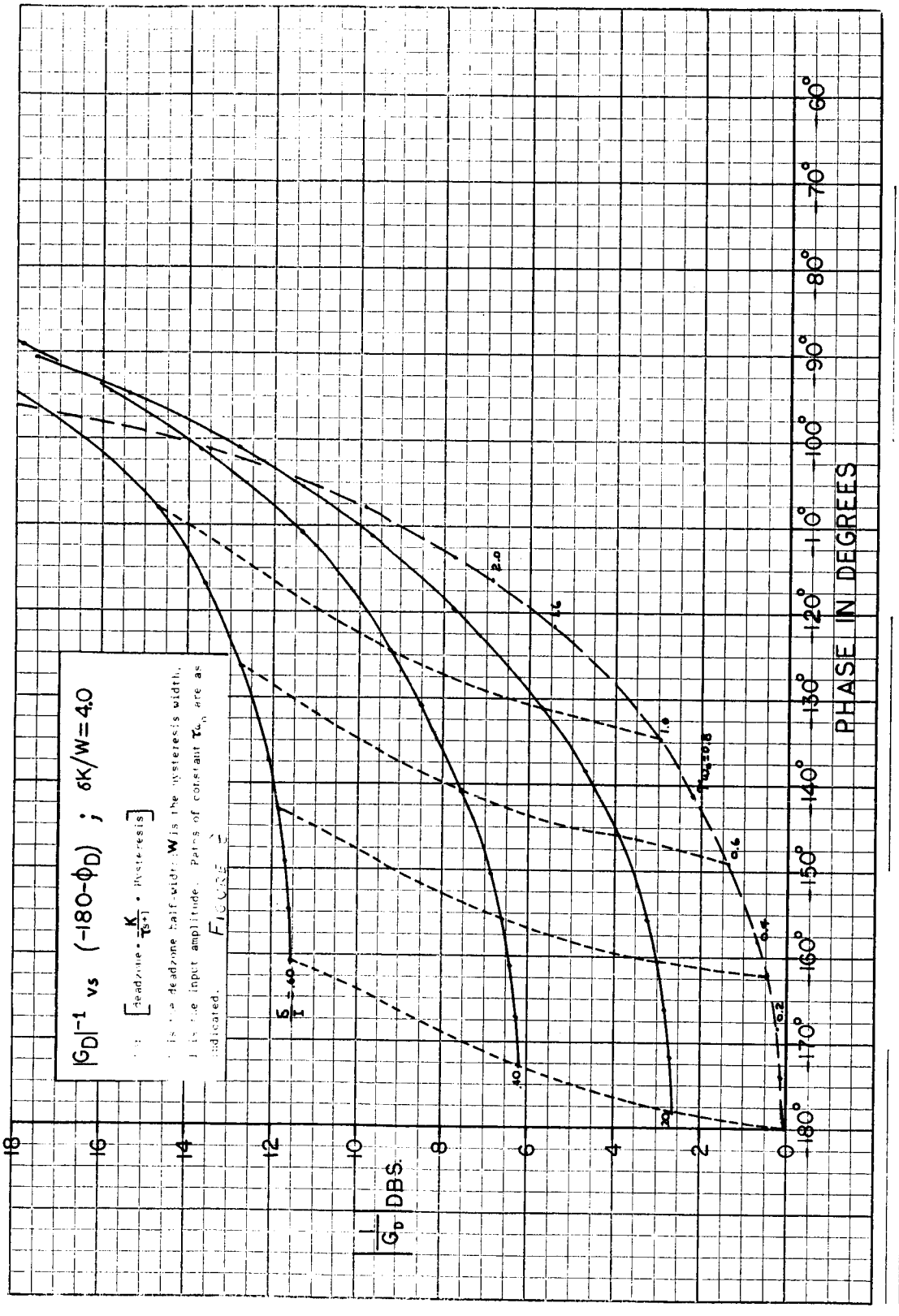
$|G_D|^{-1}$ vs $(-180-\phi_D)$; $\delta K/W = 4.0$
$\left[\text{deadzone} \cdot \frac{K}{\tau s+1} \cdot \text{Hysteresis}\right]$
$\frac{1}{|G_D|}$ DBS.
PHASE IN DEGREES
$\frac{5}{T} = 40$
40
30
20
10
2.0
1.6
1.0
0.8
0.6
0.4
0.2
18
16
14
12
10
8
6
4
2
0
+180°
+170°
+160°
+150°
+140°
+130°
+120°
+110°
+100°
+90°
+80°
+70°
+60°

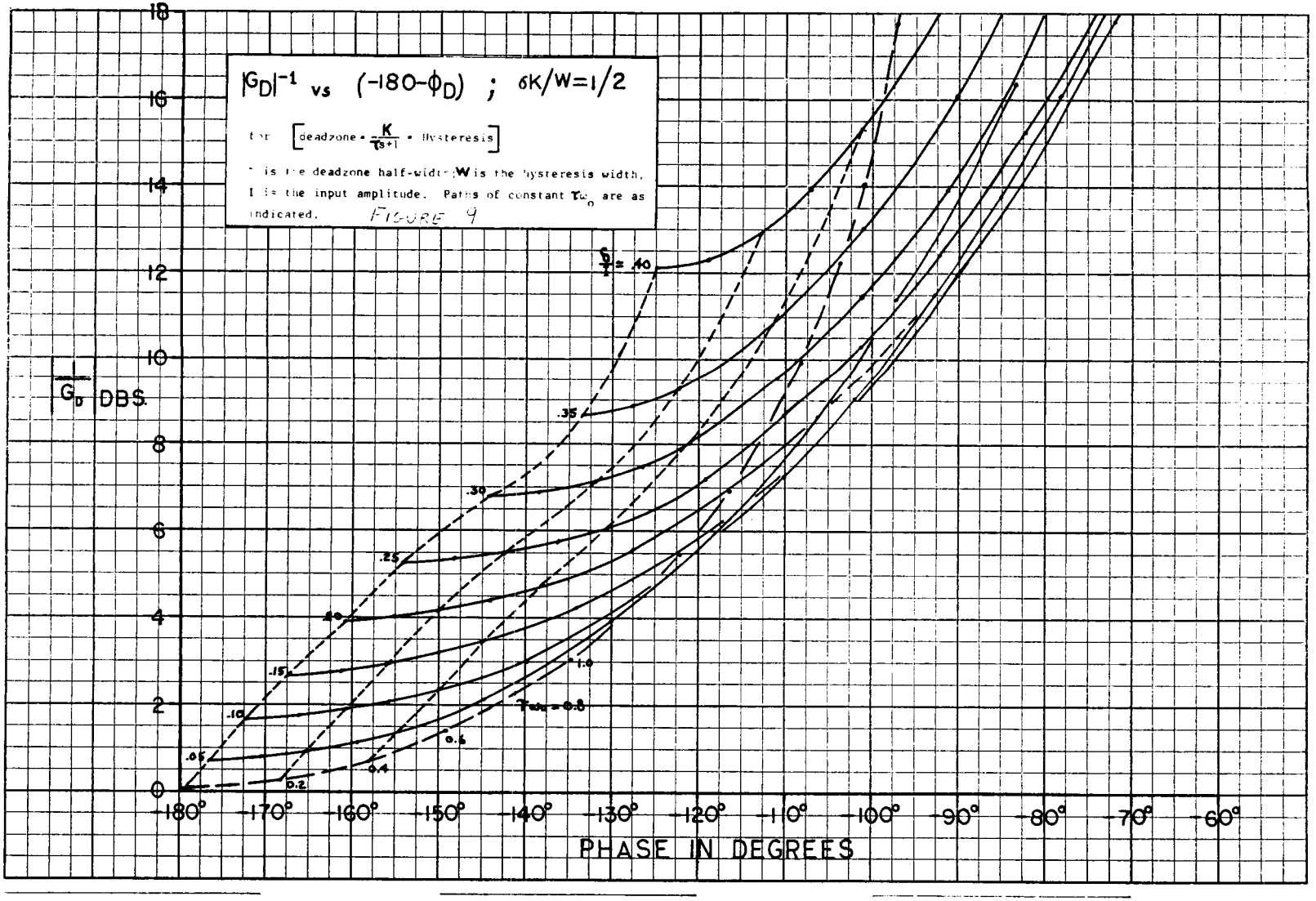
$|G_D|^{-1}$ vs $(-180-\phi_D)$; $\delta K/W = 1/2$
for [deadzone * $\frac{K}{\tau s+1}$ * Hysteresis]
δ is the deadzone half-width; W is the hysteresis width, I is the input amplitude. Paths of constant $\tau\omega_0$ are as indicated.
FIGURE 9
$\frac{1}{G_0}$ DBS
PHASE IN DEGREES
18
16
14
12
10
8
6
4
2
0
-180°
-170°
-160°
-150°
-140°
-130°
-120°
-110°
-100°
-90°
-80°
-70°
-60°
$\frac{\delta}{I}$ = .40
.35
.30
.25
.20
.15
.10
.05
1.0
$\tau\omega_0$ = 0.8
0.6
0.4
0.2

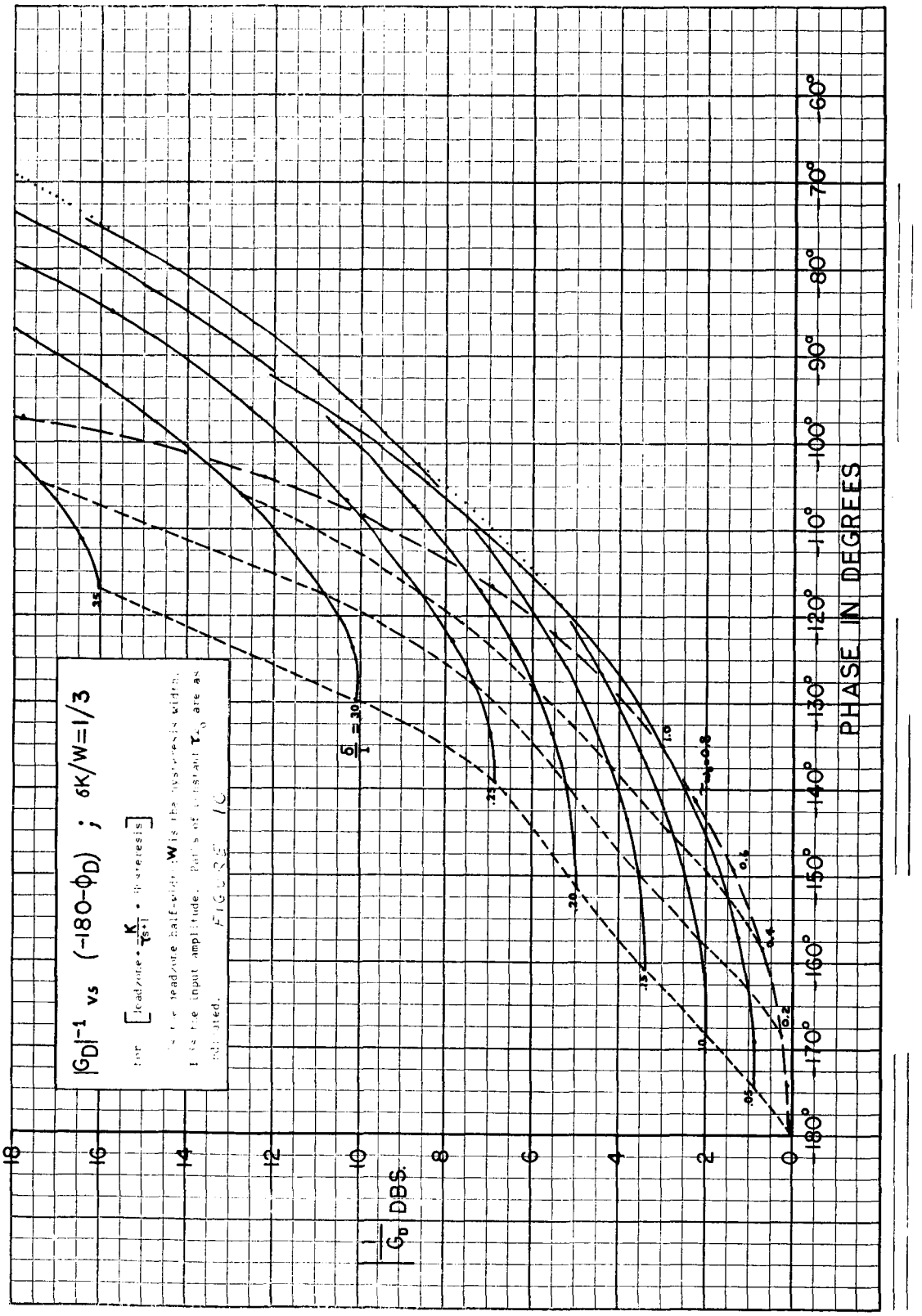
$|G_D|^{-1}$ vs $(-180-\phi_D)$; 6K/W=1/3
for $\left[\text{deadzone} \cdot \frac{K}{\tau s+1} \cdot \text{hysteresis}\right]$
$\frac{1}{G_D}$ DBS
PHASE IN DEGREES
$\frac{\delta}{I}=30$
25
20
15
10
.5
.4
.2
$\tau_0=0.8$
1.0
0.5
0.4
0.2
0.1
18
16
14
12
10
8
6
4
2
0
-180°
-170°
-160°
-150°
-140°
-130°
-120°
-110°
-100°
-90°
-80°
-70°
-60°

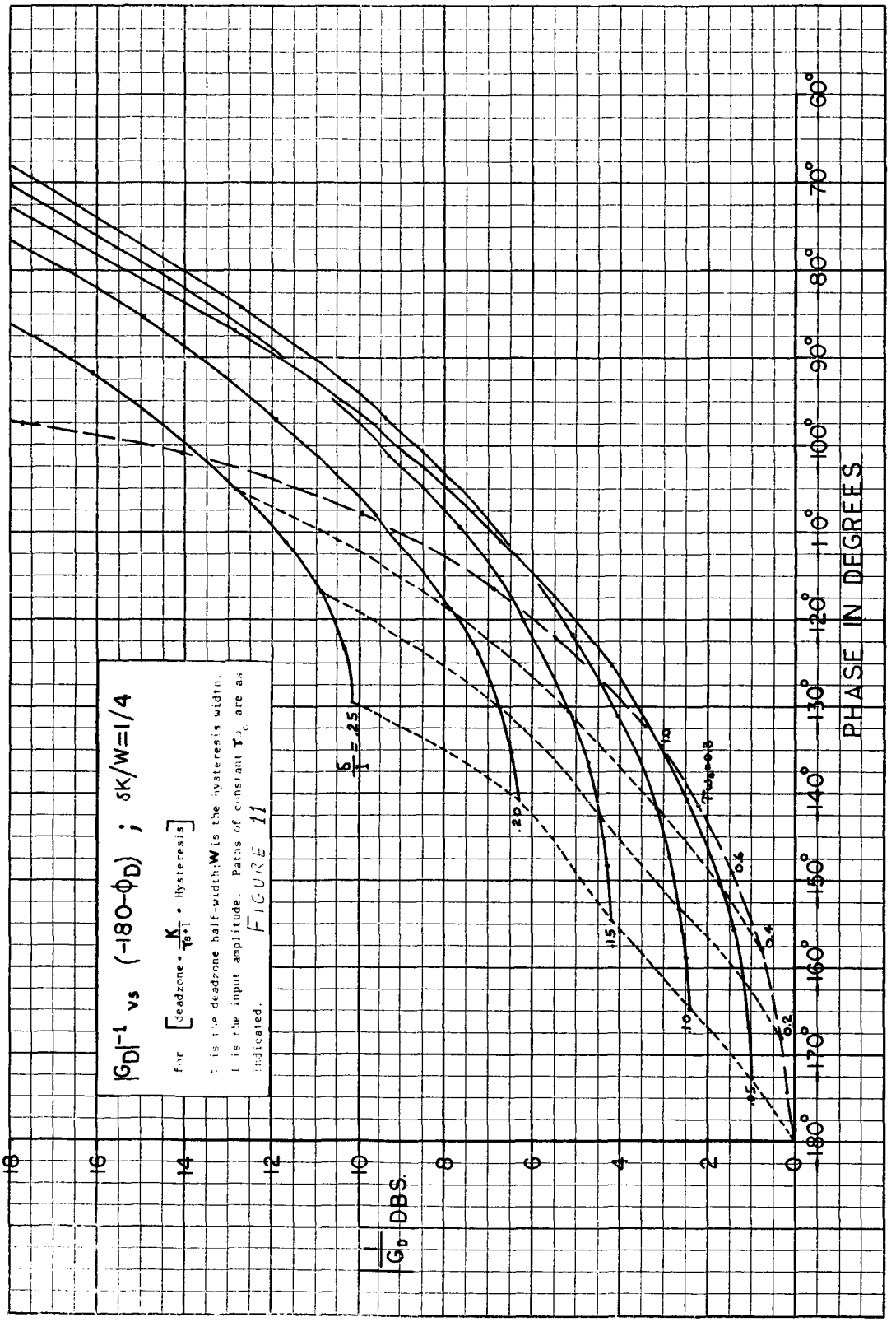
$|G_D|^{-1}$ vs $(-180-\phi_D)$; $\delta K/W=1/4$
for $\left[\text{deadzone} \cdot \frac{K}{\tau s+1} \cdot \text{Hysteresis}\right]$
δ is the deadzone half-width; W is the hysteresis width.
L is the input amplitude. Paths of constant τ_c are as indicated.
FIGURE 11
$\frac{1}{|G_D|}$ DBS.
PHASE IN DEGREES
$\frac{\delta}{L}=.25$
.2P
.15
.1
.05
.5
.4
.3
.2
.1
$\tau_c=0$

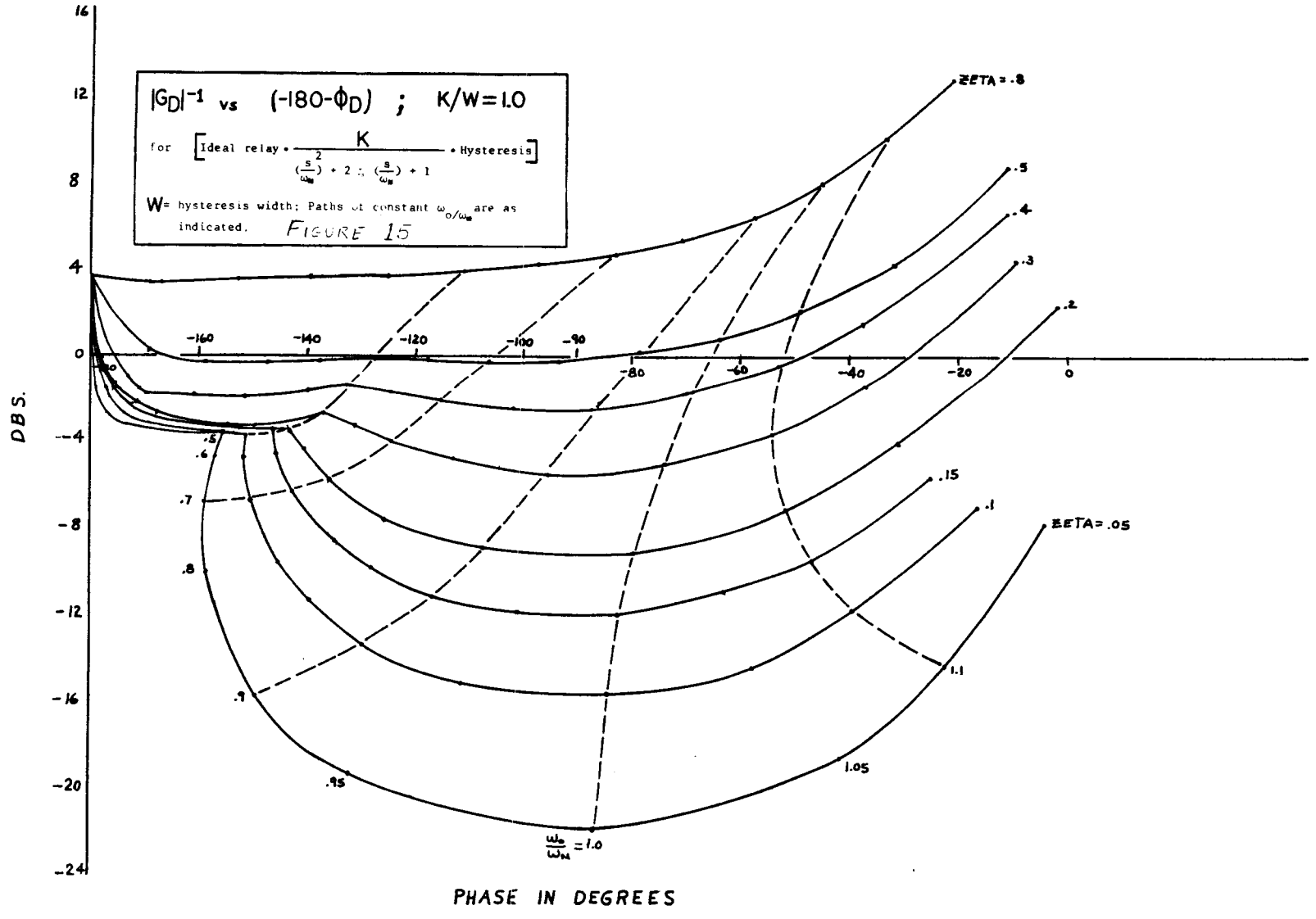
$|G_D|^{-1}$ vs $(-180-\phi_D)$; K/W=1.0
for [Ideal relay • $\frac{K}{(\frac{s}{\omega_n})^2 + 2\zeta(\frac{s}{\omega_n}) + 1}$ • Hysteresis]
W= hysteresis width; Paths of constant ω_o/ω_n are as indicated.
FIGURE 15
ZETA = .8
.5
.4
.3
.2
.15
.1
ZETA = .05
.6
.7
.8
.9
.95
1.1
1.05
$\frac{\omega_o}{\omega_n} = 1.0$
16
12
8
4
0
-4
-8
-12
-16
-20
-24
-160
-140
-120
-100
-80
-60
-40
-20
0
DBS.
PHASE IN DEGREES

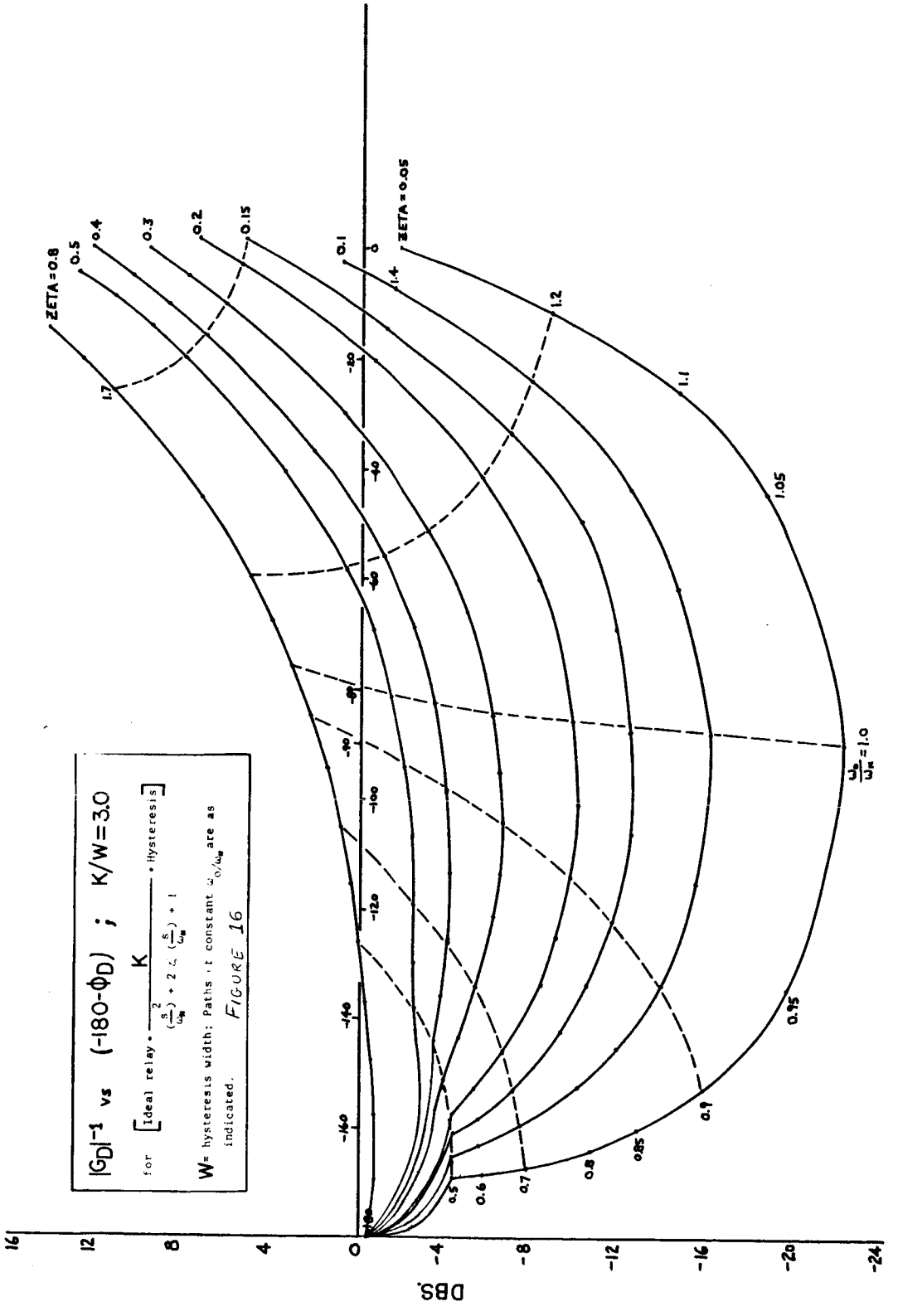
$|G_D|^{-1}$ vs $(-180-\phi_D)$; K/W=3.0
for [ideal relay - $\frac{K}{(\frac{s}{\omega_n})^2 + 2\zeta(\frac{s}{\omega_n}) + 1}$ · Hysteresis]
W= hysteresis width; Path constant ω_o/ω_n are as indicated.
FIGURE 16
ZETA=0.8
0.5
0.4
0.3
0.2
0.15
0.1
ZETA=0.05
1.7
1.4
1.2
1.1
1.05
$\frac{\omega_o}{\omega_n}$=1.0
0.95
0.9
0.85
0.8
0.7
0.6
0.5
DBS.
PHASE IN DEGREES

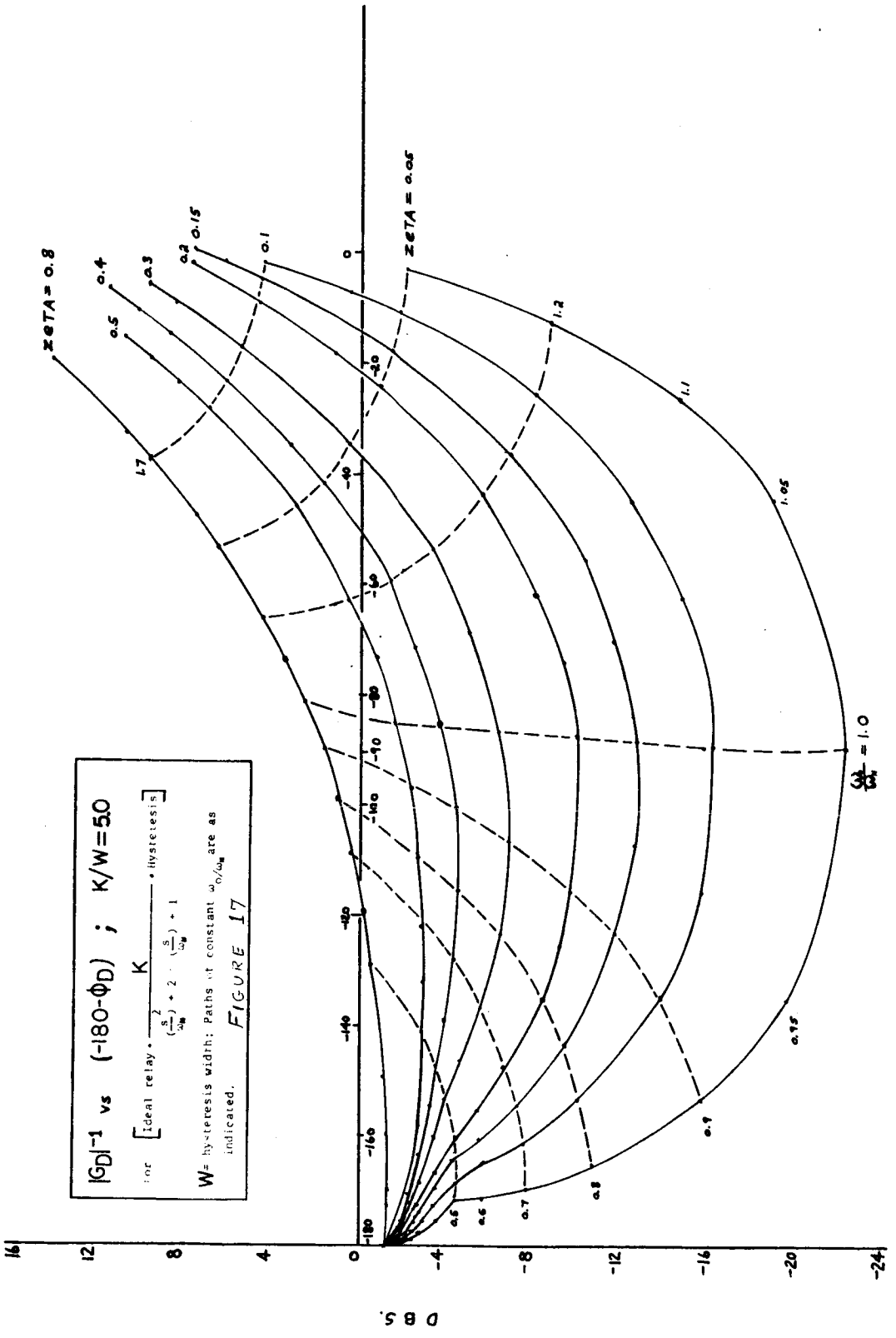

$|G_D|^{-1}$ vs $(-180-\Phi_D)$; K/W=50

for $\left[\text{ideal relay} \cdot \frac{K}{(\frac{s}{\omega_n})^2 + 2\zeta(\frac{s}{\omega_n}) + 1} \cdot \text{hysteresis}\right]$

W= hysteresis width; Paths at constant ω_σ/ω_n are as indicated.

FIGURE 17

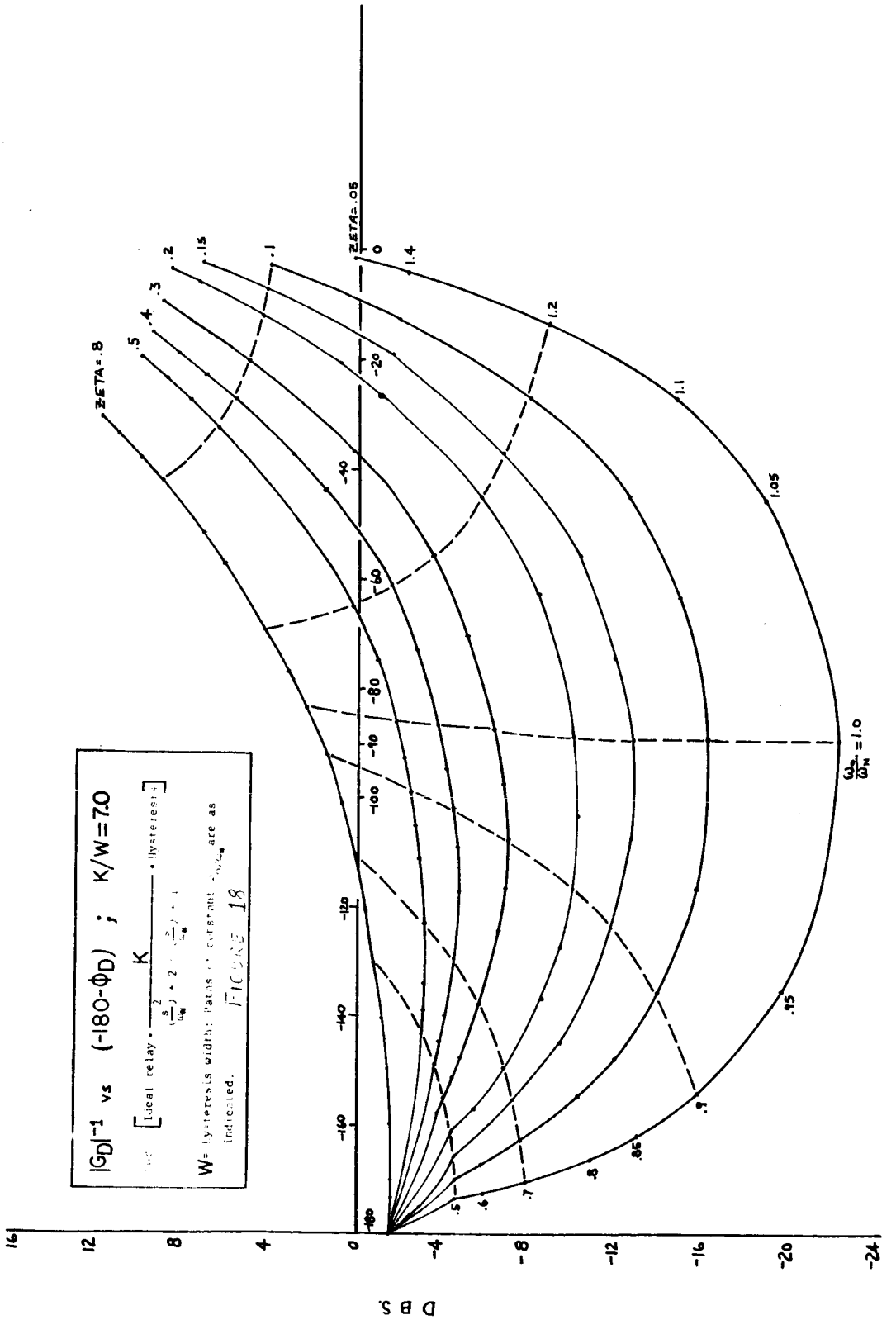
$|G_D|^{-1}$ vs $(-180-\Phi_D)$; K/W=7.0
[Ideal relay + K/(...)² + 2(...) + 1 • Hysteresis]
W= Hysteresis width; Paths of constant ... are as indicated.
FIGURE 18
ZETA=.8
.5
.4
.3
.2
.15
.1
ZETA=.05
0
1.4
1.2
1.1
1.05
1.0
.95
.9
.85
.8
.7
.6
.5
-20
-40
-60
-80
-100
-120
-140
-160
-180
16
12
8
4
0
-4
-8
-12
-16
-20
-24
DBS.
PHASE IN DEGREES

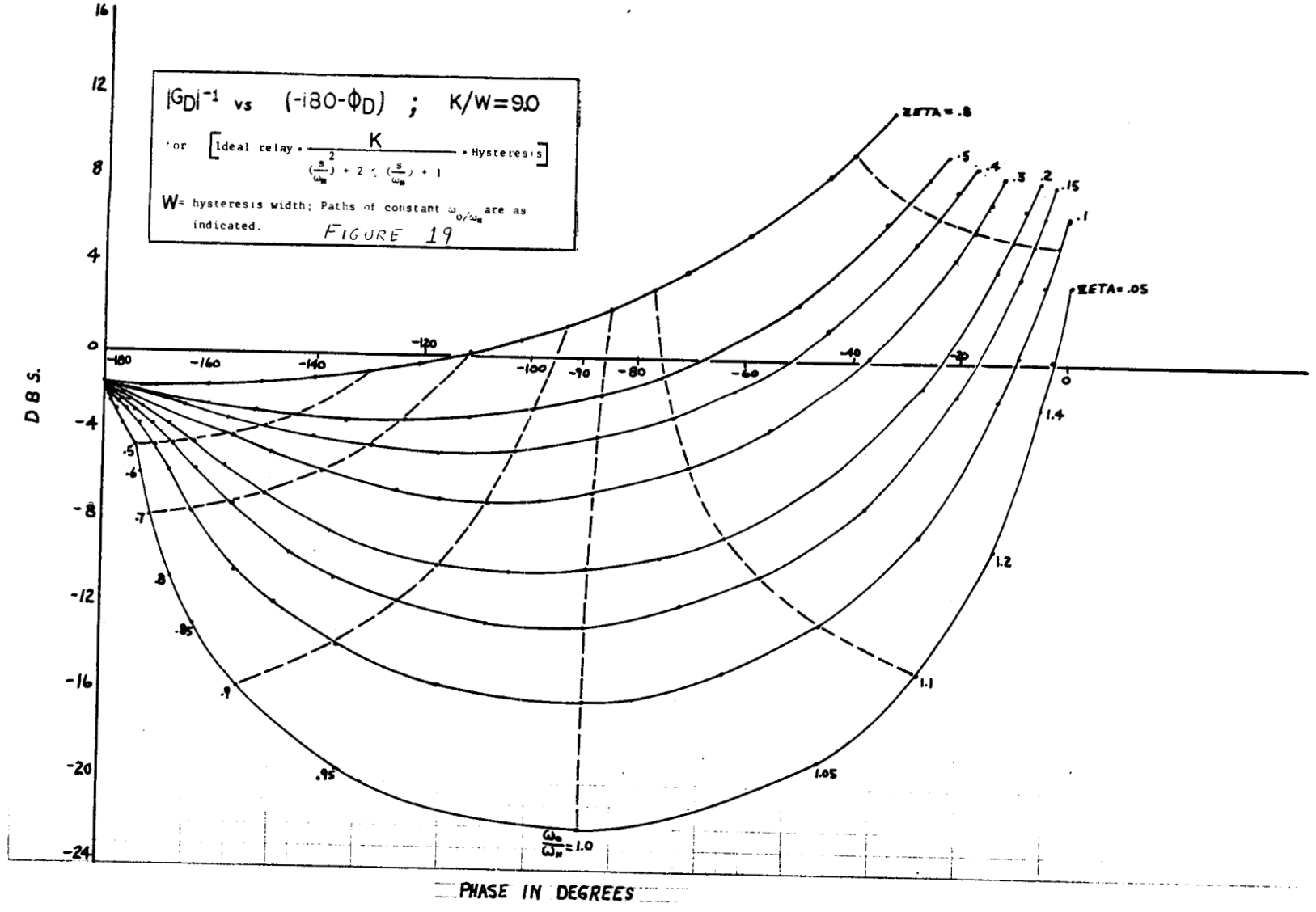
$|G_D|^{-1}$ vs $(-180-\Phi_D)$; K/W=9.0
for [Ideal relay • $\frac{K}{(\frac{s}{\omega_n})^2 + 2\zeta(\frac{s}{\omega_n}) + 1}$ • Hysteresis]
W= hysteresis width; Paths of constant ω_0/ω_n are as indicated.
FIGURE 19
ZETA=.8
.5
.4
.3
.2
.15
.1
ZETA=.05
1.4
1.2
1.1
1.05
.95
.9
.85
.8
.7
.6
.5
16
12
8
4
0
-4
-8
-12
-16
-20
-24
DBS.
-180
-160
-140
-120
-100
-90
-80
-60
-40
-20
0
$\frac{\omega_0}{\omega_n}=1.0$
PHASE IN DEGREES

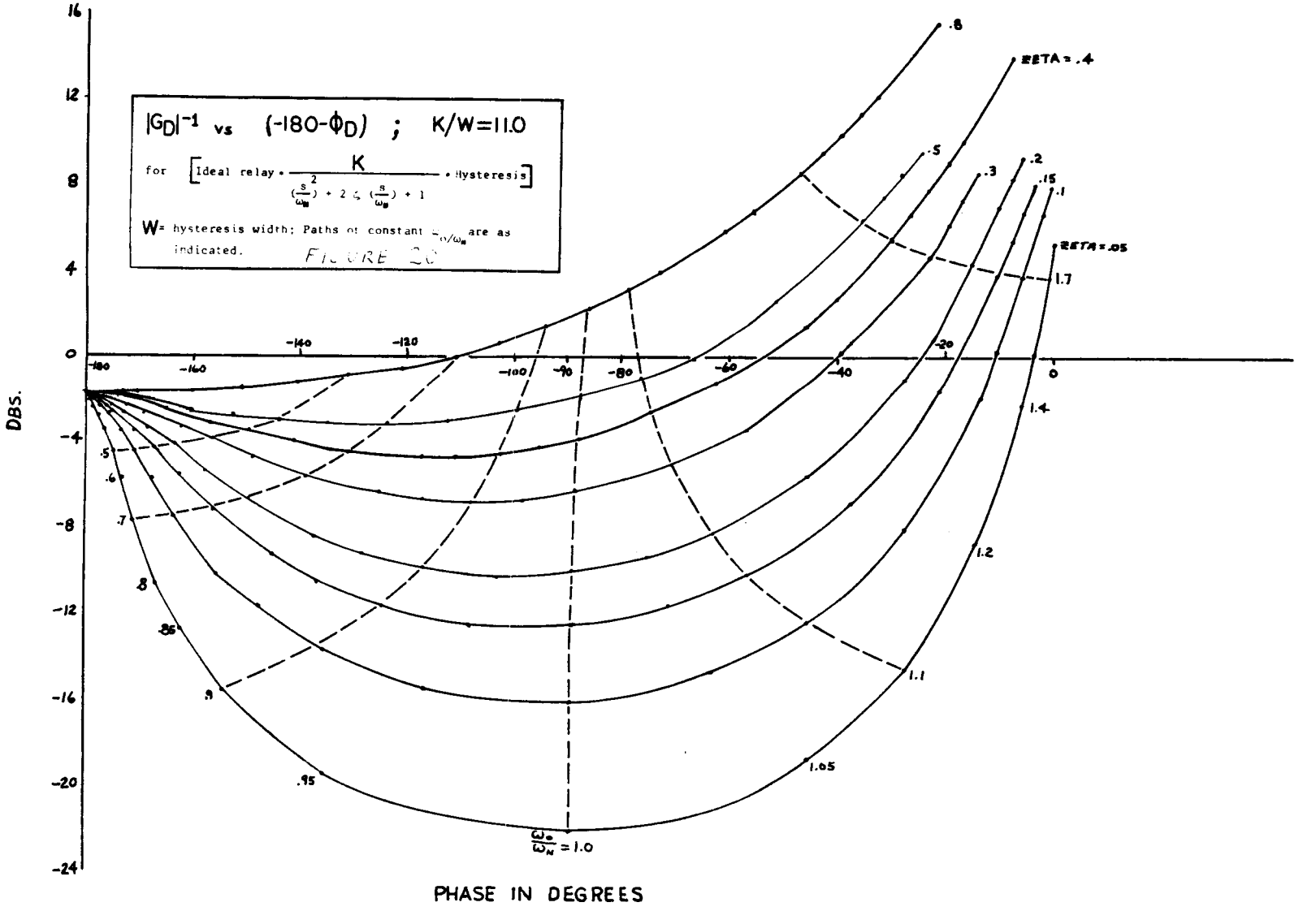
$|G_D|^{-1}$ vs $(-180-\Phi_D)$; K/W=11.0
for [Ideal relay • $\frac{K}{(\frac{s}{\omega_n})^2 + 2\zeta(\frac{s}{\omega_n}) + 1}$ • Hysteresis]
W= hysteresis width; Paths of constant ω/ω_n are as indicated.
FIGURE 20
ZETA = .4
ZETA = .05
DBS.
PHASE IN DEGREES
$\frac{\omega_o}{\omega_n} = 1.0$

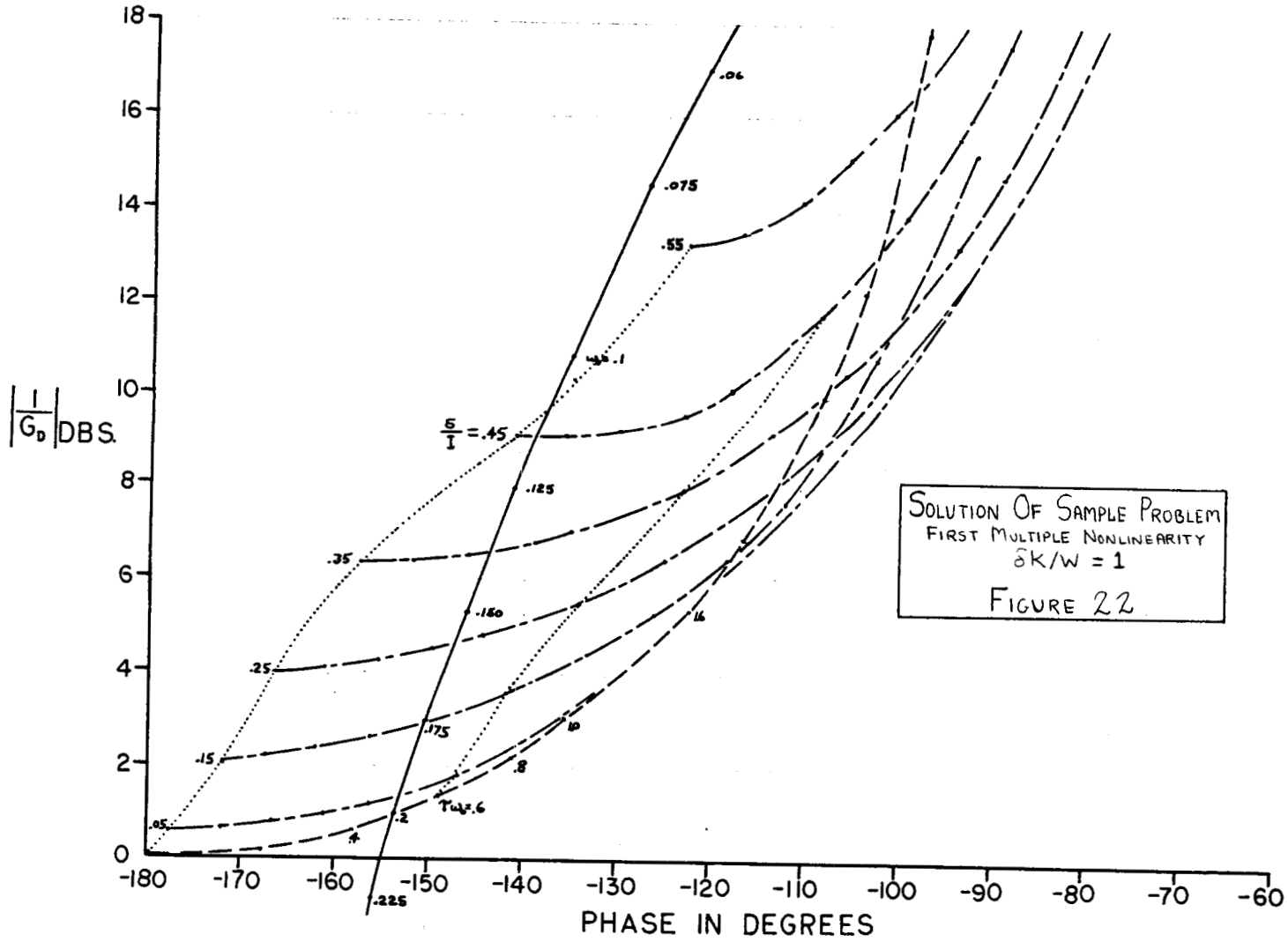

SOLUTION OF SAMPLE PROBLEM
FIRST MULTIPLE NONLINEARITY
$\delta K/W = 1$

FIGURE 22

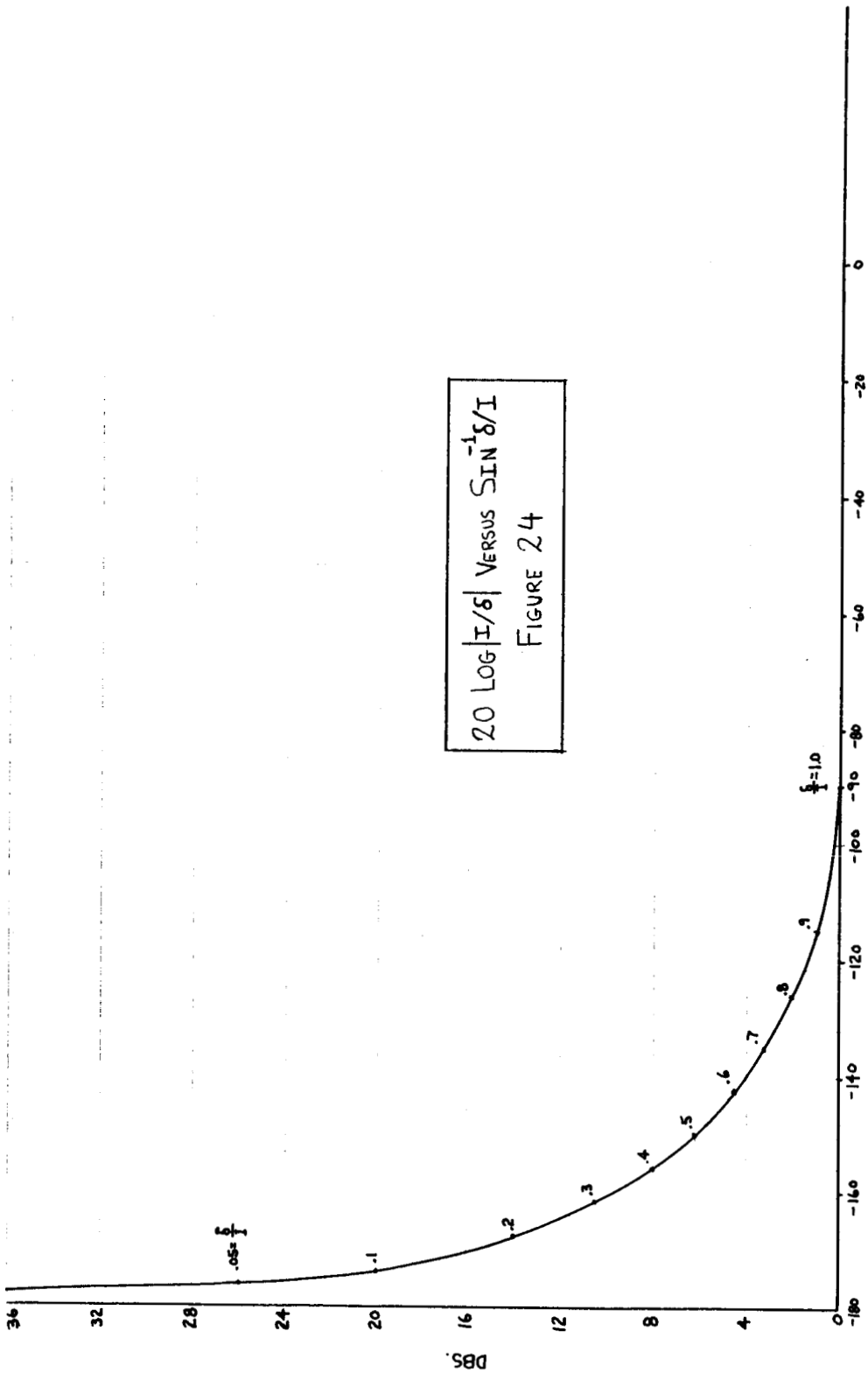

20 LOG |I/δ| VERSUS SIN^{-1} δ/I
FIGURE 24

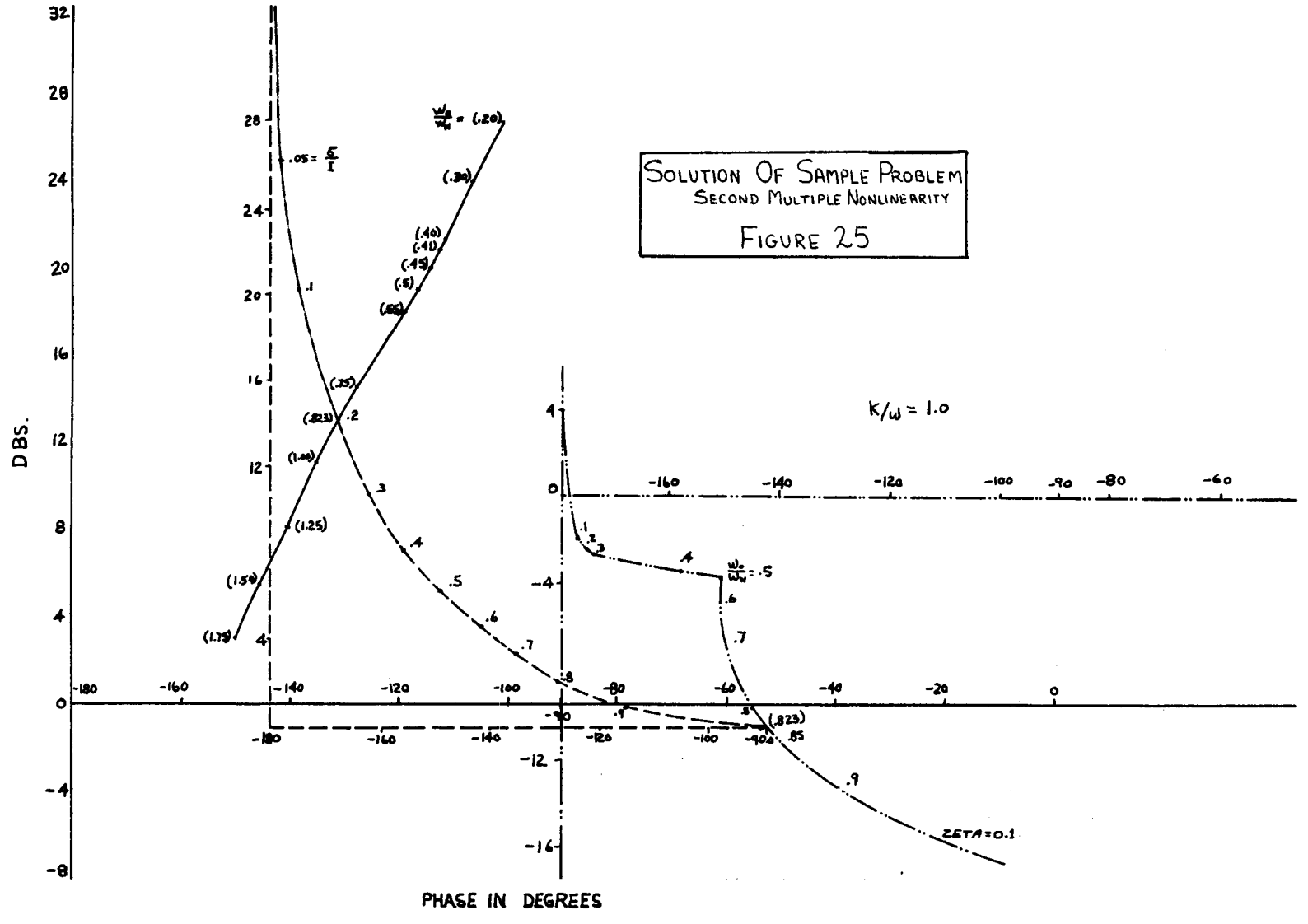
SOLUTION OF SAMPLE PROBLEM
SECOND MULTIPLE NONLINEARITY
FIGURE 25
K/ω = 1.0
DBS.
PHASE IN DEGREES
ZETA=0.1

APPENDIX I

COMPUTATION OF y(t), FIRST MULTIPLE NONLINEARITY

While deriving the describing function of the First Multiple Nonlinearity of a deadzone followed by a first order linear block and backlash, it is necessary to find the steady state output of the nonlinearity when excited by a sinusoidal signal. Let the steady state output of the deadzone nonlinearity be given by x(t) and let $x_1(t)$ represent only one cycle of this output. The steady state output of the first order linear block is denoted by y(t) and is computed as follows:

$$X_1(s) = \frac{I\,\omega_o \cos\beta}{s^2+\omega_o^2}\left[e^{-as}+e^{-bs}-e^{-cs}-e^{-ds}\right] + \frac{\delta}{s}\left[-e^{-as}+e^{-bs}+e^{-cs}-e^{-ds}\right] +$$

$$\frac{\delta s}{s^2+\omega_o^2}\left[e^{-as}-e^{-bs}-e^{-cs}+e^{-ds}\right]$$

where $a = \beta/\omega_o$, $b = (\pi-\beta)/\omega_o$, $c = (\pi+\beta)/\omega_o$, $d = (2\pi-\beta)/\omega_o$.

$$y_c(t) = \mathcal{L}^{-1}\, X_1(s)\, H(s) = K\ \mathcal{L}^{-1}\frac{X_1(s)}{(\tau s+1)}$$

$$\frac{y_c(t)}{K} = u(t-a)\left[\frac{I\,\omega_o\cos\beta}{\frac{1}{\tau^2}+\omega_o^2}\left[e^{-(t-a)/\tau}-\cos\omega_o(t-a)+\frac{\sin\omega_o(t-a)}{\tau\omega_o}\right] +\right.$$

$$\left.\frac{\delta}{(1+\tau^2\omega_o^2)}\left[\cos\omega_o(t-a)+\omega_o\tau\,\sin\omega_o(t-a)-e^{-(t-a)/\tau}\right] -\delta(1-e^{-(t-a)/\tau})\right]$$

$$+\ u(t-b)\left[\frac{I\,\omega_o\cos\beta}{\frac{1}{\tau^2}+\omega_o^2}\left[e^{-\frac{t-b}{\tau}}-\cos\omega_o(t-b)+\frac{\sin\omega_o(t-b)}{\tau\omega_o}\right] +\right.$$

$$\frac{\delta}{(1+\tau^2\omega_o^2)}\left[\cos\omega_o(t-b)+\omega_o\tau\sin(t-b)-e^{-\frac{t-b}{\tau}}\right]-\delta\left(1-e^{-\frac{t-b}{\tau}}\right)\Bigg]$$

$$+\,u(t-c)\left[\frac{I\,\omega_o\cos\beta}{\frac{1}{\tau^2}+\omega_o^2}\left[e^{-(t-c)/\tau}-\cos\omega_o(t-c)+\frac{\sin\omega_o(t-c)}{\tau\omega_o}\right]+\right.$$

$$\left.\frac{\delta}{1+\tau^2\omega_o^2}\left[\cos\omega_o(t-c)+\omega_o\tau\sin\omega_o(t-c)-e^{-(t-c)/\tau}\right]-\delta(1-e^{-(t-c)/\tau})\right]$$

$$y_t(t) = \text{Residue of } \frac{X_1(s)\,H(s)}{(1-e^{-2\pi s/\omega_o})}\,e^{st} \text{ at } s = -\frac{1}{\tau}$$

$$\frac{y_t(t)}{K} = \left[\left[\frac{I\,\omega_o\cos\beta}{\tau(\frac{1}{\tau^2}+\omega_o^2)}\right](e^{a/\tau}+e^{b/\tau}-e^{c/\tau}-e^{d/\tau})\right.$$

$$-\left[\frac{\delta}{\tau^2(\frac{1}{\tau^2}+\omega_o^2)}\right](e^{a/\tau}-e^{b/\tau}-e^{c/\tau}+e^{d/\tau})$$

$$\left.+\,\delta\,(-e^{a/\tau}+e^{c/\tau}-e^{d/\tau}+e^{b/\tau})\right]\frac{e^{-t/\tau}}{1-e^{\frac{2\pi}{\omega_o\tau}}}$$

From which

$$y(t) = y_c(t) - y_t(t)$$

APPENDIX II

COMPUTATION OF z(t), FIRST MULTIPLE NONLINEARITY

When the first multiple nonlinearity is excited by a sinusoidal signal, the expression for the steady state output y(t) of the linear block H(s), was derived in Appendix I.

Since y(t) had to be solved for various values of $\tau\omega_o$ and I, it seemed necessary to use a digital computer to compute y(t) for every run. The computation of z(t) the output of the nonlinearity, from y(t) was incorporated in the same digital program and numerical techniques of integration were used to derive the describing function.

$$A_1 = \frac{2}{\pi} \int_o^{\pi} z(t) \cos \omega_o t \, d\omega_o t \quad \text{and} \quad B_1 = \frac{2}{\pi} \int_o^{\pi} z(t) \sin \omega_o t \, d\omega_o t$$

$$\text{and } \left| G_D(I\ \omega_o) \right| = \frac{(A_1^{\,2} + B_1^{\,2})^{\frac{1}{2}}}{I} \quad \text{and } \phi = \text{Arctan } (A_1/B_1)$$

$$\left| \frac{1}{G_D\ (I,\ \omega_o)} \right| \text{DBS} = 20 \log \left| \frac{1}{G_D\ (I,\ \omega_o)} \right|$$

APPENDIX III

DESCRIBING FUNCTION OF THE COMBINED NONLINEARITY OF DEADZONE AND BACKLASH

It is necessary to derive the describing function of the first multiple nonlinearity over the entire frequency range. For values of the excitation frequency ω_o such that $\tau\omega_o \ll 1.0$, the nonlinearities of deadzone and backlash can be considered adjacent to each other. The describing function is then derived as follows:

Let $x = \sin \omega_o t$. For $1-\delta \geq W$

$$z(t) = -W/2 \qquad 0 \leq \omega_o t \leq \beta \; ; \qquad \beta = \sin^{-1} \delta$$

$$= \sin \omega_o t - \delta - W/2 \qquad \beta \leq \omega_o t \leq \pi/2 \; ; \qquad \alpha = \sin^{-1}(1-W)$$

$$= 1 - \delta - W/2 \qquad \pi/2 \leq \omega_o t \leq \pi - \alpha$$

$$= \sin \omega_o t - \delta + W/2 \qquad \pi - \alpha \leq \omega_o t \leq \pi$$

$$A_1 = \frac{2}{\pi} \int_0^{\pi} z(t) \cos \omega_o t \, d\omega_o t \; ; \quad B_1 = \frac{2}{\pi} \int_0^{\pi} z(t) \sin \omega_o t \, d\omega_o t$$

$$A_1 = \frac{2}{\pi} \left[\int_0^{\beta} -W/2 \cos \omega_o t \, d\omega_o t + \int_{\beta}^{\pi/2} (\sin \omega_o t - \delta - W/2) \cos \omega_o t \, d\omega_o t \right.$$

$$+ \int_{\pi/2}^{\pi-\beta} (1 - \delta - W/2) \cos \omega_o t \, d\omega_o t$$

$$\left. + \int_{\pi-\alpha}^{\pi-\beta} \sin \omega_o t - \delta + W/2 \cos \omega_o t \, d\omega_o t + \int_{\pi-\beta}^{\pi} (W/2) \cos \omega_o t \, d\omega_o t \right]$$

$$= \frac{W^2 - 2W}{\pi}$$

$$B_1 = \frac{2}{\pi}\left[\int_0^{\beta} (1-W/2)\sin\omega_o t\, d\omega_o t + \int_{\beta}^{\pi/2} (\sin\omega_o t - \delta - W/2)\sin\omega_o t\, d\omega_o t\right.$$

$$+ \int_{\pi/2}^{\pi-\alpha} (1 - \delta - W/2)\sin\omega_o t\, d\omega_o t$$

$$\left. + \int_{\pi-\alpha}^{\pi-\beta} \sin\omega_o t - \delta - \omega/2 \sin\omega_o t\, d\omega_o t + \int_{\pi-\beta}^{\pi} (\omega/2)\sin\omega_o t\, d\omega_o t\right]$$

$$= \frac{2}{\pi}\left[\frac{\pi}{4} - \beta - 2\delta\cos\beta + \frac{1}{2}\sin 2\beta + (1-b)\cos\alpha - \frac{1}{4}\sin 2\alpha\right]$$

For $W/2 \leq 1 - \delta \leq W$

$$z(t) = -(1 - \delta - W/2) \qquad 0 \leq \omega_o t \leq \beta_1 \; ; \quad \beta_1 = \sin^{-1}(2\delta + W - 1)$$

$$= (\sin\omega_o t - \delta - W/2) \qquad \beta_1 \leq \omega_o t \leq \pi/2$$

$$= 1 - \delta - W/2 \qquad \pi/2 \leq \omega_o t \leq \pi$$

$$A_1 = \frac{2}{\pi}\int_0^{\pi} z(t)\cos\omega_o t\, d\omega_o t \; ; \quad B_1 = \frac{2}{\pi}\int_0^{\pi} z(t)\sin\omega_o t\, d\omega_o t$$

$$A_1 = \frac{2}{\pi}\left[\int_0^{\beta_1} -(1 - \delta - W/2)\cos\omega_o t\, d\omega_o t\right.$$

$$\left. + \int_{\beta_1}^{\pi/2} (\sin\omega_o t - \delta - W/2)\cos\omega_o t\, d\omega_o t\right.$$

$$+ \int_{\pi/2}^{\pi} (1 - \delta - W/2) \cos \omega_o t \, d\omega_o t \Bigg]$$

$$= \frac{1}{\pi} \sin^2 \beta_1 - 1$$

$$B_1 = \frac{2}{\pi} \Bigg[\int_{o}^{\beta_1} -(1 - \delta - W/2) \sin \omega_o t \, d\omega_o t$$

$$+ \int_{\beta_1}^{\pi/2} (\sin \omega_o t - \delta - W/2) \sin \omega_o t \, d\omega_o t$$

$$+ \int_{\pi/2}^{\pi} (1 - \delta - W/2) \sin \omega_o t \, d\omega_o t \Bigg]$$

$$= \frac{1}{\pi} \left[\pi/2 - \beta_1 - \cos \beta_1 \sin \beta \right]$$

$$G_D (\delta, \omega) = \sqrt{A_1^2 + B_1^2} \quad \text{and} \quad \phi = \tan^{-1} A_1/B_1$$

Various values of $G_D(\delta,\omega)$ and ϕ were obtained by writing a digital program.

APPENDIX IV

COMPUTATION OF y(t), SECOND MULTIPLE NONLINEARITY

When the second multiple nonlinearity of an ideal relay followed by a second order linear block and backlash is excited by a sinusoidal signal of frequency ω_o, then the output of the realy is a square wave having the same frequency as the excitation frequency. Therefore, the input to the second order linear block is always a square wave of the excitation frequency. The steady state output y(t) of this linear block is computed as follows:

Let $x_1(t) = x(t)$ - - - - - $o \leq \omega_o t \leq 2\pi$

$= 0.0$ - - - - - $\omega_o t > 2\pi$

Now $y(t) = y_1(t) - y_t(t)$ - - - - - - - - - - - (1)

Where $y_1(t) = \mathcal{L}^{-1} \dfrac{K\, x_1(s)}{s^2/\omega_n^2 + 2\zeta s/\omega_n + 1}$

and $y_t(t) = \sum \text{Residue of } \dfrac{x_1(s)\, K\, e^{st}}{(s^2/\omega_n^2 + 2\zeta s/\omega_n + 1)} \dfrac{1.0}{(1-e^{-2\pi s/\omega_o})}$

at $s/\omega_n = -\zeta \pm \sqrt{\zeta^2 - 1}$

But $x_1(s) = -\left[\dfrac{1}{s} - \dfrac{2}{s} e^{-\frac{\beta s}{\omega_o}} + \dfrac{2}{s} e^{-\frac{\pi+\beta}{\omega_o} s} - \dfrac{1}{s} e^{-\frac{2\pi}{\omega_o} s}\right]$

$y_1(t) = \mathcal{L}^{-1} \dfrac{-1}{s(s^2+as+1)} \left[1 - 2e^{-\frac{\beta s}{\omega_o}} - e^{-\frac{2\pi}{\omega_o} s} + 2e^{-\frac{\pi+\beta}{\omega_o} s}\right]$

Where $a = 2\zeta, \quad \omega_n = 1.0$

Now $$\frac{1}{s(s^2+as+1)} = \frac{1}{s} - \frac{s+a}{s^2+as+1}$$

$$y_1(t) = -\left[1 - Qe^{-at/2} \sin(w + \phi)\right]$$

$$+ 2\left[1 - Qe^{-a/2(t-\beta/\omega_o)} \sin(w(t-\beta/\omega_o)+\phi)\right] u(t-\beta/\omega_o)$$

$$- 2\left[1 - Qe^{-a/2(t-\frac{\pi+\beta}{\omega_o})} \sin\left[w(t-\frac{\pi+\beta}{\omega_o})+\phi\right]\right] u(t-\frac{\pi+\beta}{\omega_o})$$

Where $$Q = \frac{1}{1-a^2/4}$$

$$w = (1-a^2/4)^{\frac{1}{2}}$$

$$\phi = \text{Arc tan } \frac{(1-a^2/4)^{\frac{1}{2}}}{a/2}$$

$$y_t(t) = \sum \frac{-1}{s(s^2+as+1)} \frac{(1-2e^{-\frac{\beta s}{\omega_o}} + 2e^{-\frac{\pi+\beta}{\omega_o}s} - e^{-\frac{2\pi}{\omega_o}s}) e^{st}}{(1-e^{-\frac{2\pi s}{\omega_o}})}$$

at $\quad s = -a/2 + jw$

and $\quad s = -a/2 - jw$

$$y_t(t) = \sum \frac{-1}{s(s^2+as+1)} \left[1 - \frac{2(1-e^{-\frac{\pi s}{\omega_o}}) e^{-\beta/\omega_o s}}{(1-e^{-\frac{2\pi s}{\omega_o}})}\right] e^{st}$$

$$= \sum \frac{-1}{s(s^2+as+1)} \left[1 - \frac{2e^{-\frac{\beta s}{\omega_o}}}{1+e^{-\pi s/\omega_o}}\right] e^{st}$$

$$y_t(t) = \frac{-a/2+jw+a}{2jw}\left[1 - \frac{2e^{-\beta(-a/2+jw)/\omega_o}}{1+e^{-\pi(-a/2+jw)/\omega_o}}\right] e^{(-a/2+jw)t}$$

$$+ \frac{(-a/2-jw+a)}{-2jw}\left[1 - \frac{2e^{-\beta(-a/2-jw)/\omega_o}}{1+e^{-\pi(-a/2-jw)/\omega_o}}\right] e^{(-a/2-jw)t}$$

$$y_t(t) = e^{-\frac{a}{2}t}\left[\frac{a}{2w}\left[\sin wt - 2\,\frac{e^{\frac{\beta a}{2\omega_o}}\sin w(t-\beta/\omega_o)+e^{\frac{a}{2}(\frac{\pi+\beta}{\omega_o})}\sin w(t-\beta/\omega_o+\pi/\omega_o)}{(1+2e^{\pi a/\omega_o}\cos\frac{w\pi}{\omega_o}+e^{\pi a/\omega_o})}\right]\right.$$

$$\left. + \left[\cos wt - 2\,\frac{e^{\frac{\beta a}{2\omega_o}}\cos w(t-\beta/\omega_o)+e^{\frac{a}{2}(\frac{\pi+\beta}{\omega_o})}\cos w(t-\beta/\omega_o+\pi/\omega_o)}{(1+2e^{\pi a/\omega_o}\cos\frac{w\pi}{\omega_o}+e^{\pi a/\omega_o})}\right]\right]$$

and then $y(t) = y_1(t) - y_t(t)$.

APPENDIX V

COMPUTATION OF z(t), SECOND MULTIPLE NONLINEARITY

When the second multiple nonlinearity is excited by a sinusoidal signal, the expression for the steady state output y(t) of the second order linear block is derived in Appendix I. Since y(t) had to be computed for various values of ω_o/ω_n and zeta, a digital program was written. From the expression of y(t), z(t) the output of the backlash element was computed by modifying the same digital program. Numerical techniques of integration were used to find the fundamental component in z(t). From this a family of describing functions was generated.

$$A_1 = \frac{2}{\pi} \int_o^{\pi} z(t) \cos \omega_o t \, d\omega_o t \quad ; \quad B_1 = \frac{2}{\pi} \int_o^{\pi} z(t) \sin \omega_o t \, d\omega_o t$$

$$G_D = \sqrt{A_1^{\,2} + B_1^{\,2}} \text{ and } \phi = \text{Arc tan } (A_1/B_1)$$

$$\left|\frac{1}{G_D}\right| \text{dbs} = 20 \log \left(\frac{1}{|G_D|}\right)$$

APPENDIX VI

DESCRIBING FUNCTION OF THE COMBINED NONLINEARITY OF RELAY AND BACKLASH

It is necessary to find the describing function of the second multiple nonlinearity over the entire frequency range. For values of ω_o such that $\omega_o/\omega_n \ll 1.0$, the relay nonlinearity and the backlash nonlinearity can be considered adjacent to each other. The describing function of this combined nonlinearity was derived as follows:

$$x(t) = \sin \omega_o t$$

$$z(t) = (1-W/2) \quad o \leq \omega_o t \leq \pi$$

$$= - (1-W/2) \quad \pi \leq \omega_o t \leq 2\pi$$

$$A_1 = \frac{1}{\pi} \int_o^{\pi} (1-W/2) \cos \omega_o t \, d\omega_o t - \frac{1}{\pi} \int_{\pi}^{2\pi} (1-W/2) \cos \omega_o t \, d\omega_o t$$

$$= 0.0$$

$$B_1 = \frac{1}{\pi} \int_o^{\pi} (1-W/2) \sin \omega_o t \, d\omega_o t - \frac{1}{\pi} \int_{\pi}^{2\pi} (1-W/2) \sin \omega_o t \, d\omega_o t$$

$$= - \frac{1}{\pi} (1-W/2) (-1 \ -1) + \frac{1}{\pi} (1-W/2) (1 + 1)$$

$$= \frac{4}{\pi} (1-W/2)$$

$$G_D = \frac{4}{\pi} (1-W/2)$$

APPENDIX VII

ANALOG COMPUTER SIMULATION I

An analog computer simulation of the sample problem discussed in Chapter IV was used to varify the analytical results. The block diagram of the sample problem containing first multiple nonlinearity is shown in Figure 29, while Figure 30 represents its analog computer simulation. Table XIV indicates the analog computer results as well as the analytical data.

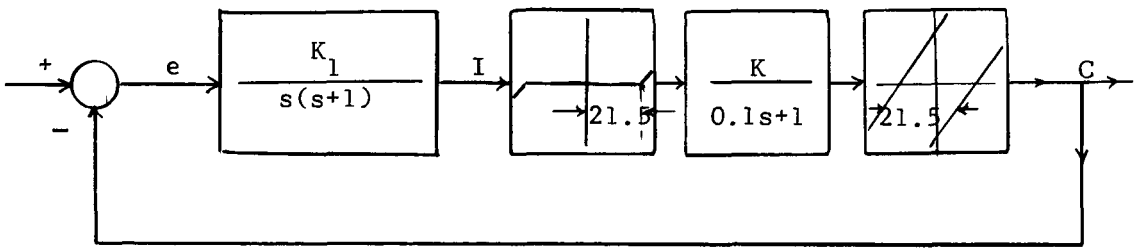

Figure 29 - Block Diagram of the Sample Problem Containing First Multiple Nonlinearity

TABLE XIV

The Analog Results Versus Analytical Results, First Multiple Nonlinearity

No. of run	SYSTEM PARAMETER		ANALYTICAL DATA				ANALOG DATA	
			Fig. No.	δ/I	LIMIT CYCLE		LIMIT CYCLE	
	δK/W	K_1			Frequency rad./sec.	Amplitude I	Frequency rad./sec.	Amplitude I
1	1.0	5.0	5	0.41	1.25	52.5	1.25	52.5
2	1.0	8.0	5	0.25	2.02	86.0	2.02	86.0
3	0.5	10.0	9	0.23	1.55	93.0	1.55	93.0
4	2.0	3.0	6	0.59	1.0	36.5	1.065	38.0
5	2.0	5.0	6	0.38	2.0	56.5	2.02	57.0

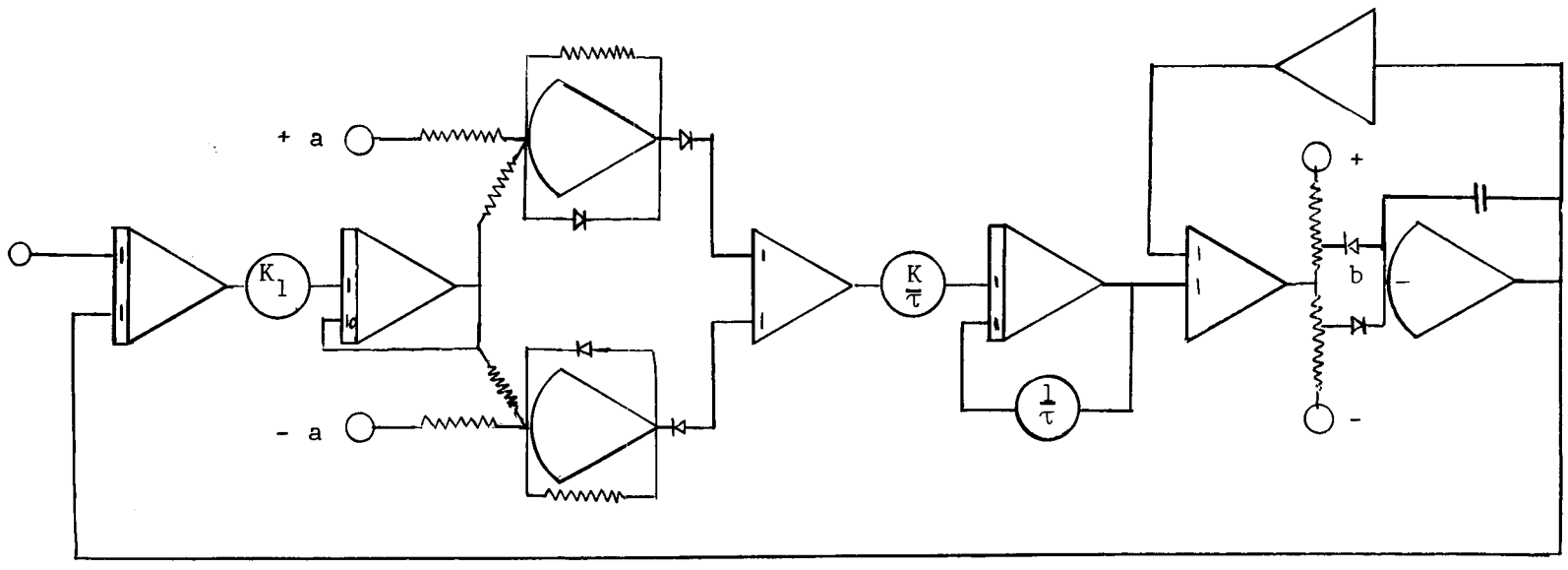

Figure 30 - Analog Computer Simulation of the Sample Problem Shown in Figure 29

Note:- $a = \delta = b = W = 21.5$ units

$\tau = 0.1$

$K_1 = 5, 3, 10, 8$

$K = 1, 0.5, 2.0$

APPENDIX VIII

ANALOG COMPUTER SIMULATION II

An analog computer simulation was used to varify the analytical results obtained in Chapter IV for the sample problem containing second multiple nonlinearity. The block diagram of the sample problem is shown in Figure 31, while Figure 32 represents its analog simulation. The results of the analog simulation and their comparison with the analytical results is presented in Table XV.

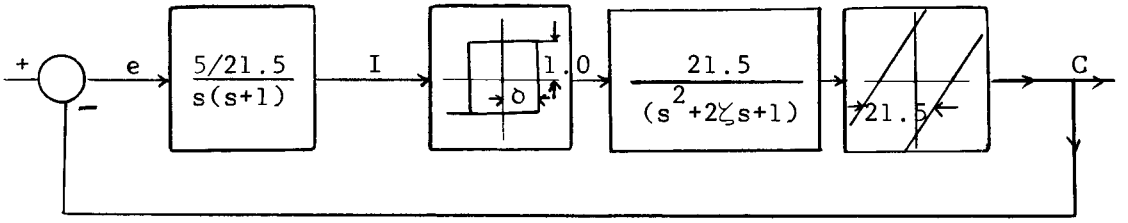

Figure 31 - Block Diagram of the Sample Problem Containing Second Multiple Nonlinearity

TABLE XV

The Analog Results Versus Analytical Results, Second Multiple Nonlinearity

SYSTEM PARAMETER		ANALYTICAL DATA		ANALOG DATA	
ZETA	δ	FREQUENCY rad./sec.	AMPLITUDE	FREQUENCY rad./sec.	AMPLITUDE
0.1	10	0.42	16.15	0.42	16.15
0.1	7	0.512	13.4	0.512	13.4
0.1	5	0.685	12.5	0.685	12.5
0.1	3	0.823	15.0	0.823	15.1
0.4	10	0.331	16.55	0.331	19.0
0.4	7	0.377	13.85	0.337	16.0
0.4	5	0.415	12.05	0.415	13.5
0.4	3	0.475	11.0	0.4745	11.6
0.8	10	0.218	13.5	0.218	16.5
0.8	7	0.26	10.5	0.2565	13.2
0.8	5	0.29	11.9	0.2925	12.0
0.8	3	0.34	9.1	0.337	9.6

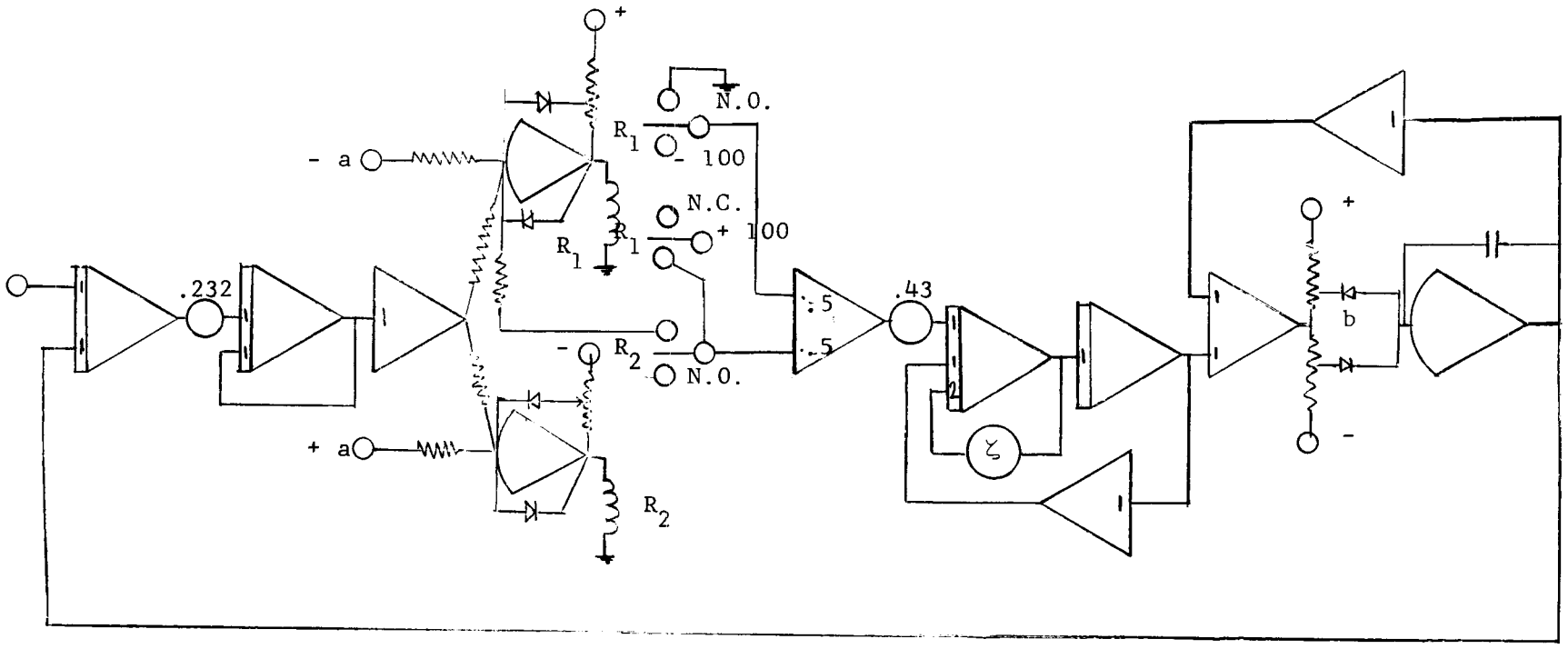

Figure 32 - Analog Computer Simulation of the Sample Problem Shown in Figure 31

Note:- b = W = 21.5 units

K = 21.5

a = δ = 10, 7, 5, and 3 units

ζ = 0.1, 0.4, and 0.8

REFERENCES

1. R. J. Kochenburger, "A Frequency Response Method for Analyzing and Synthesizing Contactor Servomechanisms," AIEE Transactions, Volume 69, Part I, 1950. Pages 270-284.

2. E. Calvin Johnson, "Sinusoidal Analysis of Feedback-Control Systems Containing Nonlinear Elements," AIEE Transactions, Volume 71, Part II, 1952. Pages 169-181.

3. M. V. Mathews, "A Method for Evaluating Nonlinear Servomechanisms," Volume 74, Part II, 1955. Pages 114-123.

4. J. G. Truxal, Control System Synthesis, McGraw-Hill Book Company, Inc., 1955. Pages 566-567.

5. J. J. D'Azzo and C. H. Houpis, Feedback Control System Analysis and Synthesis, McGraw-Hill Book Company, Inc., 1960. Pages 432-433.

6. Thaler and Pastel, Analysis and Design of Nonlinear Feedback Control System, McGraw-Hill Book Company, Inc., 1962. Pages 141-142 and pages 177-179.

7. R. Sridhar, "A General Method for Deriving the Describing Functions for a Certain Class of Nonlinearities," IRE Transactions on Automatic Control, Volume AC-5. Pages 135-141, 1960.

8. R. J. Kochenburger, "Limiting in Feedback Control Systems," AIEE Volume 72, Part II, 1953. Pages 180-192.

9. L. M. Vallese, "Comparison of Backlash and Hysteresis Effects in Second Order Feedback Systems," AIEE, Volume 75, Part II, 1956. Pages 240-243.

10. H. D. Grief, "Describing Function Method of Servomechanism Analysis Applied to Most Commonly Encountered Nonlinearities," AIEE, Volume 72, Part II, 1953. Page 243.

11. V. B. Haas, Jr., "Coulomb Friction in Feedback Control Systems," AIEE, Volume 72, Part II, 1953. Pages 119-123.

12. M. Y. Silberberg, "The Describing Function of an Element with Friction," AIEE, Volume 75, Part II, 1956. Pages 423-425.

13. A. D. Gronner, "The Describing Function of Backlash Followed by a Dead Zone," AIEE, Volume 77, Part II, 1958. Pages 403-409.

14. K. N. Satyendra, "Describing Functions Representing the Effect of Inertia, Backlash, and Coulomb Friction on the Stability of an Automatic Control System-1," AIEE, Volume 75, Part II, 1956. Pages 243-249.

15. E. A. Freeman, "Stability Analysis of Control System having Two Nonlinear Elements with Calculations for Saturation and Backlash," IEE, Monograph No. 53YM, July, 1962. Pages 665-675.

16. Seshu and Balabanian, Linear Network Analysis, John Wiley and Sons, Inc., Second printing, 1963. Pages 168-186.

17. S. M. Shinners, Control Systems Design, John Wiley and Sons, Inc., 1964. Pages 231-235 and Page 248.

18. J. E. Gibson, Nonlinear Automatic Control, McGraw-Hill Book Company, Inc., 1963. Pages 350-351.

19. J. E. Gibson and K. S. Prasanna-Kumar, "A New R.M.S. Describing Function for Single-Valued Nonlinearities," Proceedings IRE, Volume 49, 1961. Page 1321.

20. R. F. Finnigan, "Transient Analysis of Nonlinear Servomechanisms Using Describing Function with Root Locus Techniques," Ph.D. Thesis, University of Illinois, Urbana, Illinois, 1957.

21. L. T. Prince, Jr., "A Generated Method of Determining the Closed Loop Frequency Response of Nonlinear Systems," Transactions AIEE, Part II, September, 1954.

22. E. Levension, "Some Saturation Phenomena in Servomechanisms with Emphasis on the Tachometer Stabilized System," Transactions AIEE, Part II, March, 1953.

23. J. C. Hill, "Closed Loop Response of Nonlinear Systems by a Functional Transformation Approach," IRE Transactions on Automatic Contrl, Volume AC-7, No. 4, 1962. Pages 30-45.

24. R. C. Boyer, "Sinusoidal Signal Stabilization," Master's Thesis, Purdue University, Lafayette, Indiana, January, 1960.

25. J. C. West, J. L. Douce, R. K. Livesly, "The Dual-Input Describing Function and Its Use in the Analysis of Nonlinear Feedback Systems," Proceedings of IEE, Volume 103, Part B, 1956. Pages 463-473.